



저작자표시-비영리-변경금지 2.0 대한민국

이용자는 아래의 조건을 따르는 경우에 한하여 자유롭게

- 이 저작물을 복제, 배포, 전송, 전시, 공연 및 방송할 수 있습니다.

다음과 같은 조건을 따라야 합니다:



저작자표시. 귀하는 원저작자를 표시하여야 합니다.



비영리. 귀하는 이 저작물을 영리 목적으로 이용할 수 없습니다.



변경금지. 귀하는 이 저작물을 개작, 변형 또는 가공할 수 없습니다.

- 귀하는, 이 저작물의 재이용이나 배포의 경우, 이 저작물에 적용된 이용허락조건을 명확하게 나타내어야 합니다.
- 저작권자로부터 별도의 허가를 받으면 이러한 조건들은 적용되지 않습니다.

저작권법에 따른 이용자의 권리는 위의 내용에 의하여 영향을 받지 않습니다.

이것은 [이용허락규약\(Legal Code\)](#)을 이해하기 쉽게 요약한 것입니다.

[Disclaimer](#)

Master's Thesis of Science in Agriculture

**Stimulation of Dopamine D1 receptor enhances
the therapeutic function of mesenchymal stem cells
in acute kidney injury**

도파민 D1 수용체가 활성화된 중간엽줄기세포가 급성신장손상
회복에 미치는 영향에 대한 연구

February 2021

Seo Yeon Jo

**Department of International Agricultural Technology
Graduate School of International Agricultural Technology
Seoul National University**

**Stimulation of Dopamine D1 receptor enhances
the therapeutic function of mesenchymal stem cells
in acute kidney injury**

A thesis

submitted in partial fulfillment of the requirements to the faculty
of Graduate School of International Agricultural Technology
for the Degree of Master of Science in Agriculture

By

Seo Yeon Jo

Supervised by

Prof. Tae Min Kim

Major of International Agricultural Technology
Department of International Agricultural Technology
Graduate School of International Agricultural Technology
Seoul National University

December 2020

Approved as a qualified thesis
for the Degree of Master of Science in Agriculture
by the committee members

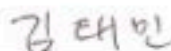
Chairman

Joonghoon Park, Ph.D.



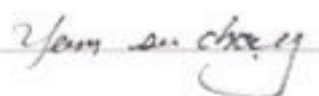
Member

Tae Min Kim, Ph.D.



Member

Su Cheong Yeom, Ph.D.



Abstract

Acute kidney injury (AKI) remains a major health problem worldwide. The reasons include significant mortality, morbidity, and lack of treatment. During recent decades, studies showed that mesenchymal stem cells (MSCs) can become an alternative tool for AKI management. However, low survival rate *in vivo* due to excessive oxidative stress at the injury site, and poor homing capacity, limit their clinical therapeutic potentials. Therefore, a successful strategy in the transplantation of hUC-MSCs would be to prevent oxidative stress-induced apoptosis. Fenoldopam (FD), which is a selective dopamine receptor 1 agonist, has been reported that the anti-oxidant effects of D1-like receptors are exerted by inhibiting the pro-oxidant enzyme, NADPH oxidase, and stimulate anti-oxidant enzymes, heme oxygenase-1 (HO-1). However, the the effect of FD on UC-MSCs in reducing oxidative damage remains unexplored.

This study aimed to determine whether the activation of the dopamine D1 receptor by FD can reduce oxidative damage in MSCs. Further, the therapeutic effect of FD-primed MSCs in acute renal dysfunction was assessed in cisplatin-induced AKI model. As results, I found that FD-stimulated MSCs showed better outcome in proliferation, differentiation

potential and self-renewal capacity. Moreover, H₂O₂-induced cell damage was reduced by FD treatment, as shown by decreased production of reactive oxygen species and apoptosis rate. Biochemical analysis showed that the expression of Bcl-2-associated X protein (BAX) was reduced, and that mitochondria membrane potential (Ψ_m) was maintained through activating NRF2 and CREB by stimulating PI3K/AKT and ERK1/2 pathway.

Furthermore, After administration of cisplatin, blood urea nitrogen (BUN) and creatinine (Crea) levels, necrosis of proximal tubules, Ki-67 and f4/80 positive cells increased in mice. However, Cisplatin-induced AKI mice treated with FD-primed MSCs showed a significant reduction in all the above index. Conclusively, FD-primed MSCs has potential to become an alternative way for reducing AKI.

Key words: dopamine receptors, oxidative stress, mesenchymal stem cells, acute kidney injury

Student number: 2019-20975

Contents

Abstract.....	i
Contents.....	iii
List of Tables.....	vi
List of Figures.....	vii
List of Abbreviations.....	viii
1. Introduction.....	1
1.1 Characteristic and therapeutic potential of MSCs.....	1
1.2 Major challenges of MSCs cell therapy.....	2
1.3 The Mechanism of reactive oxygen species generation.....	3
1.4 Anti-oxidant defense mechanism of dopamine D1 receptor activation.....	3
1.5 Acute Kidney Injury (AKI)	4
1.6 Preclinical studies of MSC-based therapy in AKI.....	5
2. Materials and Methods.....	10
2.1 Cell culture.....	10
2.2 Cell treatments.....	10
2.3 Flow cytometry.....	11
2.4 <i>In vitro</i> differentiation	11
2.5 Analysis of differentiation potential of MSCs.....	12

2.6 Assessment of cytotoxicity using CCK-8 assay.....	13
2.7 Analysis of apoptosis.....	13
2.8 Detection of mitochondrial membrane potential (Ψ_m)	14
2.9 Measurement of ROS	14
2.10 qRT-PCR.....	11
2.11 Western blotting analysis.....	13
2.12 Immunocytochemistry.....	14
2.13 Animal model of AKI.....	14
2.14 Kidney histology and measurement of injury.....	15
2.15 Immunohistochemistry and evaluation of immunostaining.....	15
2.16 <i>In vivo</i> MSCs-homing studies.....	16
2.17 Statistical analysis.....	17
 3. Results.....	 22
3.1 Effects of on MSC viability.....	22
3.2 Comparison of characteristics of mesenchymal stem cell.....	25
3.3 FD-primed MSCs alleviated H ₂ O ₂ -induced apoptosis.....	30
3.4 FD-primed MSCs maintain Ψ_m in ROS.....	35
3.5 FD prevents intracellular ROS formation in MSCs.....	39
3.6 FD-primed MSCs stimulate the expression of HIF-1 α , HO-1, NRF2.....	42
3.7 translocation of NRF2 into the nucleus by FD.....	46
3.8 Identification of the signaling pathways.....	48
3.9 FD-primed MSCs alleviates cisplatin-induced AKI.....	56

4. Discussion.....	66
References.....	71

List of Tables

Table 1. The sequences of primers.....	16
Table 2. The antibody list used in this study	47

List of Figures

Figure 1. Mesenchymal stem cells : Mechanism of action.....	8
Figure 2. Chemical structure of FD and effects of FD on MSC viability.....	23
Figure 3. Phenotype, multilineage differentiation and CFU-F colony formation of MSCs and FD-primed MSCs.....	28
Figure 4. FD significantly reduced H₂O₂ induced apoptosis in hUC-MSCs.....	32
Figure 5. FD-primed MSCs maintain H₂O₂ mediated Ψ_m reduction.....	38
Figure 6. FD-primed MSCs scavenge intracellular ROS produced by H₂O₂ in MSCs.....	40
Figure 7. Expression of hypoxia-inducible factor (HIF)-1α, heme oxygenase (HO)-1, Nuclear factor erythroid-2-related factor 2 (NRF2).....	43
Figure 8. Effects of FD on H₂O₂-induced apoptosis related protein in mesenchymal stem cells.....	50
Figure 9. Effects of FD on the phosphorylation of AKT, ERK, and CREB in MSCs.....	52
Figure 10. Schematic diagram explaining the mechanism that effects of FD reduce ROS in MSCs.....	54
Figure 11. FD-primed MSCs improve renal recovery in an AKI.....	59

List of Abbreviations

AKT	Protein kinase B
BAX	BCL-2-associated X protein
BCL-2	B-cell lymphoma2
BSA	Bovine serum albumin
Ctrl	Control
D1DR	Dopamine receptor D1
DLS	Dynamic light scattering
ERK	Extracellular signal-regulated kinase 1/2
EVs	Extracellular vesicles
FBS	Fetal bovine serum
FD	Fenoldopam
FD-primed MSC	Fenoldopam primed Mesenchymal Stem Cells
GA	Gentamicin/amphotericin-B
GAG	Glycosaminoglycans
GEnC	Glomerular Endothelial cells
GPCR	G Protein-Coupled Receptor
GPX4	Glutathione peroxidase 4
H ₂ O ₂	Hydrogen peroxide
HIF-1 α	Hypoxia-inducible factor 1-alpha
HO-1	Heme oxygenase 1

hUC-MSCs	Human umbilical cord-derived mesenchymal stem cells
IL-6	Interleukin 6
IL-8	Interleukin 8
IP	Intraperitoneal
IV	Intravenous
MCP1	Monocyte chemoattractant protein 1
mRNA	Messenger RNA
NQO1	NAD(P)H Quinone Oxidoreductase 1
NRF2	Nuclear factor erythroid 2-related factor 2
PCR	Polymerase Chain Reaction
PI3K	phosphoinositide 3-Kinase
qPCR	Quantitative Polymerase Chain Reaction
REGM	Renal Epithelial Cell Growth Medium
RO	Retro-orbital
ROS	Reactive oxygen species
SOD	Superoxide dismutase
α -MEM	α -Minimum Essential Medium Eagle

Introduction

1.1 Characteristics and therapeutic potential of MSCs

Mesenchymal stem cells (MSCs) are non-hematopoietic[1], adult stem cells that have been isolated from Wharton's jelly from umbilical cord, adipose tissue[2], bone marrow[3]. According to the minimal criteria of the International Society for Cellular Therapy (ISCT), human MSC should be plastic-adherent when maintained in standard culture conditions. Second, MSC must express CD105, CD73 and CD90, and lack expression of CD45, CD34, CD14 or CD11b, CD79 α or CD19 and HLA-DR surface molecules. Third, MSC able to differentiate into mesenchymal lineage, such as osteoblasts, adipocytes and chondroblasts *in vitro*[4-6].

MSCs are a promising cell for regenerative medicine due to have immunosuppressive and anti-oxidant properties, and their tissue regeneration efficacy has been consistently proven in inflammatory or many degenerative diseases [7-10].

1.2 Major challenges of MSC therapy

It is reported that the biological characteristics of MSC may differ depending on the age, gender and health status of the donor as well as the method of cell isolation and culture [11, 12]. For example, the differentiation potential of MSCs was not affected by donor age or gender, but there was a difference in gene expression profile among different donors (e.g., from various donors), and also in the gender-specific inhibitory role against T cell proliferation [12]. Other study showed that MSCs derived from human adipose tissue of lean or obese donors had different potential of proliferation, migration, as well as their innate immunophenotype profile. This may be resulted from the different microenvironment within the adipose tissue, such as low oxygen levels and chronic low-grade inflammation[11].

Despite their beneficial effects, the application of MSCs is limited due to pathophysiological environmental conditions, including oxidative stress, inflammation, low oxygen levels, and restricted nutrient supply[13]. Various stress conditions trigger reduced proliferation and loss of stemness and can induce senescence, resulting in >99% cell death during the first few days following MSC transplantation[14-17]. Therefore, protection against several stress and optimization of MSC culture conditions are required to produce functional MSCs with high therapeutic efficiency. To address this issue, culture condition modification (3D culture, hypoxic condition), genetic

modification (pro-survival, anti-apoptotic, migration and anti-oxidant related gene), preconditioning (cytokine, small_molecules), cell-free MSC-based therapy have been suggested to increase the survival of MSCs[13, 18, 19].

1.3 The mechanism of reactive oxygen species generation

The redox environment regulates many physiological and pathophysiological mechanisms. The term oxidative stress can be defined as a serious disturbance of the balance between the production of pro-oxidants, or free radicals, that oxidize lipids, proteins, and DNA and the ability to detoxify intermediate metabolites easily and has been shown in a wide range of studies to contribute to the pathogenesis of many diseases[20]. The most widely studied free radicals are reactive oxygen species (ROS), which include the superoxide anion ($O_2 \cdot^-$), hydroxyl radical ($\cdot OH$), and hydrogen peroxide (H_2O_2). Mitochondrial complexes I and III, and the NADPH oxidase isoform NOX4 are major sources of ROS production during MSC differentiation[21].

1.4 Anti-oxidant defense mechanism of dopamine D1 receptor activation

D1R, D2R, and D5R have been reported to be important in maintaining a normal redox balance. In the kidney, the anti-oxidant effects of these receptors are caused by direct and indirect inhibition of pro-oxidant enzymes,

specifically, nicotinamide adenine dinucleotide phosphate, reduced form (NADPH) oxidase, and stimulation of anti-oxidant enzymes, which can also indirectly inhibit NADPH oxidase activity[22]. Fenoldopam mesylate, a benzazepine derivative, is the first selective dopamine-1 receptor agonist approved for clinical use[23]. Oxidative stress is one of the fundamental mechanisms responsible for the development of hypertension.

Dopamine, via five subtypes of receptors, plays an important role in the control of blood pressure by various mechanisms, including the inhibition of oxidative stress[24].

1.5 Acute Kidney Injury (AKI)

Kidney disease, including acute kidney injury (AKI), is one of the most significant causes of mortality and morbidity all over the world. AKI is a condition in which kidney function rapidly deteriorates within hours to days. AKI occurs in 13 million people per year worldwide[25]. AKI is common in intensive care units and requires renal replacement therapy (RRT) in severe cases of AKI, and these patients show 50-70% mortality[26]. The underlying etiologies of AKI vary significantly, and the causes of AKI can be divided into three types: pre-renal, intrinsic, and post-renal AKI. Pre-renal AKI is mainly due to the lack of volume in the body, such as severe hemorrhage, vomiting, diarrhea, and cardiac output decrease that occurs secondary to

cardiac failure. Intrinsic AKI is mainly caused by the injury to the kidney cells by nephrotoxic drugs (e.g., anti-cancer drugs and antibiotics), viral and bacteria infection, or abnormal immune system response. The main pathological findings include acute tubular necrosis (ATN), acute glomerulonephritis (AGN), and acute interstitial nephritis (AIN). Post-renal AKI is caused by the obstruction of ureter or urethra after the kidney, likewise those found in prostatic hypertrophy, bilateral renal calculi, and bladder carcinoma[27].

AKI increases the risk of CKD and end-stage renal disease(ESRD)[28, 29]. Current therapies for AKI include regular dialysis and renal replacement therapy. However, these therapies are no significant impact on overall mortality[30]. Also, as pharmacologic therapy, Low-dose dopamine for renal protection has been described. However, it is now clear that is not effective for the treatment of AKI and may even be harmful[31]. Currently, no single drug can be used for AKI due to its complex pathophysiology[32].

1.6 Preclinical studies of MSC-based therapy in AKI

A number of studies have demonstrated that various cell types can reduce AKI induced by ischemia reperfusion injury (IRI)[33, 34] or nephrotoxic drugs such as cisplatin[35, 36], glycerol[37, 38], or gentamicin[39]. Z Qiu et al. showed that eGFP-labeled MSCs injected to tail vein localized to the renal

tubule in an IRI-induced AKI model, and it was found that the number of cells expressing ICAM-1 and PMNLs was decreased, while the proliferating renal cells were increased. These results indicate that MSCs potentially decreased the inflammation in the kidney, while also promoted the survival of tubular cells[33]. Other study showed that adipose-derived MSCs was effective in alleviating inflammation and oxidative stress, and senescence-related protein (β -galactosidase, p21^{Waf1/Cip1}, p16^{INK4a}) and micro RNA(miR-29a, miR-34a) in an IRI-induced AKI model [34].

The secretome of mammalian cells can be altered by active chemical or biological compound during maintenance, a priming strategy has now being developed in cell therapy. Pretreating MSCs with resveratrol was able to reduce the progress of AKI in cisplatin-induced model. Specifically, resveratrol treatment onto MSCs promoted the secretion of platelet-derived growth factor-DD(PDGF-DD) in renal tubular cells. Also, ERK signaling was more activated, also showing that vessel growth was stimulated[40]. Other study showed that systemically injected amniotic fluid stem cells led to renal regeneration in cisplatin-induced AKI, partially via anti-oxidant activity as shown by decreased malondialdehyde (MDA) and increased level of superoxide dismutase (SOD) and glutathione (GSH)[36].

The ability to recover from acute renal failure (ARF) is largely dependent on the replacement of damaged tubular cells with functional tubular epithelium[37]. When MSCs were co-cultured with glycerol-induced ARF rat kidney tissue, MSCs differentiated into renal tubular epithelial-like cells expressing the renal markers cytokeratin 18(CK18) and aquaporin-1 (AQP1), and the homing capacity of MSCs to the injured kidney was also confirmed. These finding also showed a therapeutic effect in ARF[38]. In addition, in the gentamicin-induced AKI model, MSC overexpressing insulin-like growth factor-1 (IGF-1) showed better anti-oxidation, anti-inflammatory, and migration capacity[41]. As such, the possibility of MSCs as a therapeutic agent was validated in various AKI models, also supported by molecular and cellular mechanisms, several among which are the engraftment and subsequent differerntiation into new renal (e.g., tubular) cells. The main mechanism underlying the protective effects is commonly regarded to be its paracrine/endocrine activity that regulates immune cells, attenuate inflammation, present anti-oxidant, and anti-apoptotic effects[42, 43].

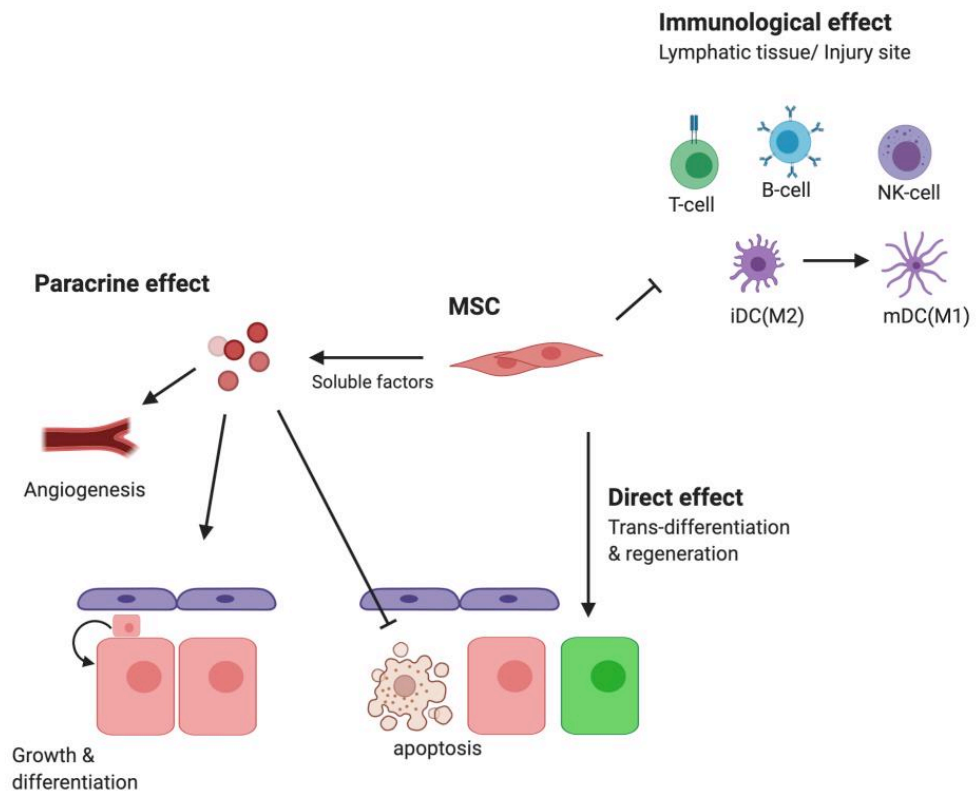


Figure 1. Mesenchymal stem cells : Mechanism of action.

MSCs can differentiate into various mesenchymal lineages to replace damaged tissue. Also, MSCs have ability to secrete soluble factors that can stimulate the growth and differentiation target cells including endothelial cells. Finally, the unique immunomodulating capacity of MSCs can help to inhibit excessive immune reaction and inflammation.

(Table adapted from [44])

2. Materials and Methods

2.1 Cell culture

Human Umbilical Cord mesenchymal stem cells (ATTC, Manassas, VA) were maintained in MEM- α (Thermo Fisher Scientific, Waltham, Massachusetts, USA) supplemented with 10 % Fetal bovine serum (FBS, atlas Biologicals, Fort Collins, USA) and 1 % Antibiotics-Antimycotics (Genedirex, Taoyuan, Taiwan). After cell growth reached 80 % confluence, hUC-MSCs were split into 1:3 by being treated with TrypLE Express (Thermo Fisher Scientific, Waltham, Massachusetts, USA).

2.2 Cell treatments

MSCs were treated with or without 3 $\mu\text{g/mL}$ FD in MEM- α for 72 h. Groups primed with FD will be referred to as FD-primed MSCs, otherwise they will be referred to as MSCs.

MSCs were seeded into six-well plates or 60mm dish. Once cell density reached 80 %, H_2O_2 (300 μM for 24 h or H_2O_2 500 μM for 6 h), was used to establish an *in vitro* oxidative stress model.

2.3 Flow cytometry

hUC-MSCs were harvested at 80 % confluency and then, Cells were resuspended 1×10^6 in 100uL of PBS containing 4 % FBS (FACS buffer). For cell surface labeling, cell suspensions were incubated at 4 °C for 1 h with the following specific primary antibodies such as CD34 Mouse anti-Human (100:1) (clone 4H11, Invitrogen, Carlsbad, CA, USA), FITC Mouse Anti-Human CD90, Clone 5E10, RUO (17:1), PE Mouse Anti-Human CD73, RUO (5:1), PE Mouse Anti-Human CD105, 266, RUO (20:1) (Biosciences, Franklin Lakes, NJ, USA). After incubation, the samples were washed three times in 1mL FACS buffer. For the unconjugated primary markers, the secondary antibody goat anti-mouse igG H&L Dylight 488 (Abcam, Cambridge, UK) was used. Collected data was analyzed by the BD FACS Canto™ II Cytometer and FACS DIVA software (Ver6.1.3, BD Bioscience, Franklin Lakes, NJ, USA)

2.4 In vitro differentiation

hUC-MSCs (passages between 7-9) were seeded in 4-well plates (SPL, KOR) at a density of $8 \times 10^4/15 \mu\text{L}$ in MEM- α with 10 % FBS under 5 % CO₂ condition at 37 °C. For chondrogenic differentiation, After 16 h, the culture medium was replaced with StemPro chondrogenesis medium (Thermo Fisher

Scientific, Waltham, MA, USA). The medium was changed every 3 days. For Osteogenic differentiation, cells were seeded in 4-well plates at density of 2×10^4 and maintained at 37 °C and 5 % CO₂. After 16 h, the culture medium was removed, and the StemPro osteogenesis differentiation medium (Thermo Fisher Scientific, Waltham, MA, USA) was added. Their differentiated potential was examined after 2 weeks of differentiation. Chondrogenic differentiation was examined by staining with Alcian Blue staining kit (Lifeline Cell Technology, Frederick, MD, USA) to identify sulfated proteoglycans deposits. Osteogenic differentiation was examined by staining with 2 % Alizarin Red staining kit (Lifeline Cell Technology, Frederick, MD, USA) to identify the Ca²⁺ deposits.

2.5 Analysis of differentiation potential of MSCs

MSCs were prepared as described above in the presence or absence of FD. GAG content with ECMs was quantified using an Alcian blue stain. Briefly, MSCs were rinsed in distilled H₂O, and then incubated overnight in 0.1N HCl containing 0.1 % Alcian blue. The ECM rinsed three times in distilled H₂O, extracted using 200 µL of 0.1 N HCl, and absorbance was measured at 620 nm. The presence of mineral in enzymes[45]. Quantitative analysis of Alizarin Red staining was performed. Briefly, 10 % acetic acid was added and agitated gently for 30 min, and the supernatant was collected. After washing with 200

μL of 10 % acetic acid, they were collected in the same tube. After adding 250 μL of mineral oil to the tube, the samples were incubated at 85°C for 10 min, followed by being incubated in ice. After spin down at 12000 rpm for 15 min, 250 μL of supernatant was mixed with 100 μL of ammonium hydroxide. The Absorbance was measured at 405 nm.

2.6 Assessment of cytotoxicity using CCK-8 assay

Cell viability was analyzed using CCK-8 (Dojindo Laboratories, Kumamoto, Japan) according to the manufacturer's instruction. Briefly, hUC-MSCs were plated into 96 wells. For detecting the cytotoxicity of FD or H₂O₂, hUC MSCs were incubated with FD (0-50 μg/mL) or H₂O₂ (300-400 μM) in MEM-α medium for 24 h-96 h. Thereafter, the medium was replaced with 100 μL fresh medium and 10 μL CCK-8 solution was added. After further incubation for 2-3 hours at 37 °C, the amount of formazan generated by cellular dehydrogenases activity was measured 450 nm by a microplate reader (TECAN, Mannedorf, Swotzerland).

2.7 Analysis of apoptosis

Cell apoptosis induced by H₂O₂ was analyzed using the Annexin V-FITC Apoptosis Detection Kit I (BD Bioscience, Franklin, NJ, USA). In brief, hUC-MSCs were seeded at 1x10⁵ cells/ml in 6-well culture plates and

incubated w/wo FD for 3 day and incubated with 500 μM H_2O_2 for 6 h. Following treatment, both adherent and floating cells were harvested, washed twice in cold PBS, and resuspended in 500 μL of binding buffer. The number of cells was counted and divided into 4 groups by $1 \times 10^5/100 \text{ uL}$. The four groups are divided into (PI-, FITC-), (PI+, FITC-), (PI-, FITC+), (PI+, FITC+), Annexin V-FITC solution (5 μL) and PI (5 μL) were added to each group and the cell were incubated for 30min in the dark. The cells were analyzed BD FACS DIVA software (Ver 6.1.3, BD Biosciences, Franklin, NJ, USA)

2.8 Detection of mitochondrial membrane potential (Ψm)

JC-1 was used to measure the change in Ψm . Briefly, following treatment, Cells were washed with cold PBS, stained with 4 μM JC-1 and incubated for 45min at 37 $^\circ\text{C}$. Subsequently, cells were washed twice with ice-cold PBS and resuspended 1x Imaging Buffer solution. Analysis was performed using a BD FACS canto TM II Cytometer and FACS DIVA software (Ver6.1.3, BD Bioscience, Franklin Lakes, NJ, USA)

2.9 Measurement of ROS.

In microscopic analysis, cells were washed and incubated with 10 μM DCF-DA for 30min. After incubation, cells were washed twice with PBS.

Fluorescent intensity (excitation / emission = 495 / 520 nm) was measured by Cytation 5 (BioTek, VT, USA). In flow cytometry, intracellular ROS was evaluated using 2',7'-Dichlorofluorescein diacetate (Sigma-Aldrich, Merck Millipore). Briefly, following treatment, both adherent and floating cells were harvested, the cells were washed and then incubated with 20 μ M DCF-DA in serum-free culture medium for 30 min at 37 °C in the dark. The cells were washed and then analyzed BD FACS DIVA software (Ver 6.1.3, BD Biosciences, Franklin, NJ, USA).

2.10 qRT-PCR

hUC-MSCs were harvested and then lysis at Trizol (Invitrogen, Carlsbad, CA, USA). The concentration of total RNA was measured using DeNovix DS-11 (Denovix, Wilmington, DE, USA). RNA was reverse transcribed with cDNA synthesis Kit (Philekorea, Daejeon-si, Korea), and qPCR was performed using the Accupower 2X GreenStar qPCR Master Mix (Bioneer, Daejeon-si, Korea) in CFX96 Touch Real-Time PCR Detection System (Bio RAD, Hercules, California). After the expression of each gene was normalized against Gapdh, their relative expression was analyzed by the $2^{-\Delta\Delta C_t}$ method[46].

Table 1. The sequences of primers used for confirming anti-oxidant effects of hUC-MSCs

Target gene	Sequences
<i>Gapdh</i>	F:5'-GAGTCAACGGATTTGGTCGT-3' R:5'-TTGATTTTGGAGGGATCTCG-3'
<i>Nrf-2</i>	F:5'- TACTCCCAGGTTGCCACAA-3' R:5'-CATCTACAAACGGGAATGTCTGC-3'
<i>HO-1</i>	F:5'-TCTCTTGGCTGGCTTCCTTAC-3' R:5'-GCTTTTGGAGGTTTGAGACA-3'
<i>NQO1</i>	F:5'-AGGCTGGTTTGAGCGAGTTC-3' R:5'-ATTGAATTCGGGCGTCTGCTG-3'
<i>SOD</i>	F:5'-TGGCCGATGTGTCTATTGAA-3' R:5'-GGGCCTCAGACTACATCCAA-3'
<i>GPx1</i>	F:5'-CTCTTCGAGAAGTGCGAGGT-3' R:5'-TCGATGTCAATGGTCTGGAA-3'
<i>GPx4</i>	F:5'-GCACATGGTTAACCTGGACA-3' R:5'-CTGCTTCCCGAACTGGTTAC-3'
<i>Catalase</i>	F:5'-GCCTGGGACCCAATTATCTT-3' R:5'-GAATCTCCGCACTTCTCCAG-3'

2.11 Western blot analysis.

Cells were washed with ice-cold PBS, lysed with RIPA lysis buffer and centrifuged at 12,000 x g for 15min at 4°C. The protein concentration was evaluated by the Pierce™ BCA Protein Assay Kit (Thermo Fisher Scientific, Waltham, MA, USA). Equal amounts of total protein samples (15-20 µg) were separated by 10% sodium dodecyl sulfate-polyacrylamide gel electrophoresis (SDS-PA GE) and transferred to nitrocellulose membranes. After being blocked with 5% non-fat dry milk in Tris-buffered saline and Tween-20 buffer, The primary antibodies for anti-phosphorylated (p)-AKT1/2/3, AKT1/2/3, (p)-ERK1/2, ERK1/2, (p)-CREB, CREB, BAX, HO-1 (SantaCruz, Dallas, TX, USA; 1:1000), CD-9 (1:2000), β-Actin (Abcam, Cambrige, UK; 1:10000) were incubated with the membrane at 4 °C overnight. After the membrane was washed three times with TBST (0.1 % Tween 20) the membranes were incubated for 1 h at room temperature with horseradish peroxidase-conjugated anti-rabbit or mouse secondary antibody (Abcam, Cambrige, UK; 1:10000). After being washed three times with TBST, the reactivity was examed by an enhanced chemiluminescence kit (Thermo Fisher Scientific, Waltham, MA, USA). The image of the membrane was taken using chemiluminescence on a Davinci-K Gel Imaging System (Davinch-K, Seoul-si, Korea). The blots were quantified using Image J (Version1.50, National Institutes of Health, Bethesda, MD, USA).

2.12 Immunocytochemistry.

7000 cells were seeded in a Poly-D-Lysine-coated Cell Culture Slide 8 well (SPL) and cultured for 24 hours. After washing for 3 times with cold PBS, cells were fixed using 4 % paraformaldehyde in PBS (pH 7.4) for 10 min at RT. For the permeabilization, the cells were incubated for 10 min with PBS containing 0.1% Triton X-100 and then washed 3 times with cold PBS, followed by blocking in 1 % BSA in PBST (PBS + 0.1 % Tween20) for 30 min. Samples were then incubated with primary antibodies overnight at 4 °C, washed 3 times with cold PBS, and then incubated with secondary antibody for 1 hour. After washing 3 times with PBS, samples were stained with 0.1 µg/mL DAPI for 1 minute. The images were analyzed and recorded under a confocal microscope (Leica TCS SP8 STED, Wetzlar, Germany).

2.13 Animal model of AKI

All animal experiments were approved by the Institutional Animal Care and Use Committee (no. SNU-190413-6-1). BALB/c mice weighing 19-23g were obtained from Koatech (PyeongTack, Korea) and maintained under specific pathogen free conditions. The mice were randomly divided into several groups. After i.p. injection of 12mg/kg cisplatin, 5x10⁵ hUC-MSCs (w/wo FD) were retro-orbitally injected. Saline-injected mouse was used as control.

Amifostine is known to prevent cisplatin-induced nephrotoxicity by scavenging ROS[47]. Therefore, amifostine was used as a control drug. All animals were sacrificed at 96 h after cisplatin injection.

2.14 Kidney histology and measurement of injury

Kidney tissues were fixed in 4 % paraformaldehyde and routinely processed for paraffin embedding. Sections were stained with hematoxylin and eosin for histological assessment. For quantification of renal injury, injury score was analyzed as described in a previous study[48]. Briefly, viable (intact tubular morphology) or necrotic (totally disrupted tubule with loss of cuboidal cells) were marked and counted in stained tissue in a 200x magnification. With these two extremes, tubules with a thin cytoplasm containing less nuclei was counted as injured ones. Tubules showing more nuclei with normal cells were counted as recovering ones. Finally, the percentage (%) of each pattern in total number of tubules was calculated.

2.15 Immunohistochemistry and evaluation of immunostaining

Immunohistochemistry was used for detection of Ki-67 and f4/80 *in vivo*. The kidney tissue slices were deparaffinized in xylene and rehydrated in descending ethanol series from 100-70 %. Then, antigen retrieval was performed according to the product description of Antigen Retrieval Buffer

(100X citrate Buffer pH 6.0) (Abcam, Cambridge, UK). The UltraVision LP Detection System HRP DAB kit (Thermo Fisher Scientific, Waltham, Massachusetts, USA) was used according to manufactures's protocol. Briefly, Slides were immersed in UltraVision Hydrogen Peroxide Block for 10 min at RT, washed four times in PBST (0.05 % Tween20), and incubated with UltraVision Protein Block for 5 min at RT. After washing four times with PBST, the slides were incubated with F4/80 (D2S9R) XP® Rabbit mAb (1:250), Ki-67 (D2H10) Rabbit mAb (1:1000) (Cell Signaling Technology, London, UK) overnight at 4°C. The slides were washed four times with PBST and incubated with Primary Antibody Enhancer for 10 min at RT, followed by an incubation with HRP Polymer for 15 min at RT. The slides were washed four times with PBST and the color was developed following incubation with 1:33 dilution of DAB Quanto Chromogen in DAB Quanto Substrate for 1 min at RT. The slides were subsequently washed four times with distilled water and counterstained in Mayer's hematoxylin (4science, Kor) for 1 min 30sec at RT, washed in running tap water and mounted. Then, slices were hydrated in ascending to ethanol series from 70-100%. Images from representative fields were obtained using an Olympus BX43 light microscope (magnification, x200; Olympus Corporation, Tokyo, Japan).

2.16 In vivo MSCs-homing studies.

To confirm the *in vivo* biodistribution of MSCs, MSCs and FD-primed MSCs were stained with lipophilic carbocyanine DiOC18(7) ('DiR') (Invitrogen, Carlsbad, CA, USA). Briefly, MSCs incubated with 10 µg/mL of DiR for 30 min at 37°C. The unbound DiR was removed by washing three times with ice cold PBS and labeled cells were resuspend in 100µL ice-cold PBS.

Prepared cells were transplanted into AKI mouse via retro orbital injection.

Fluorescence images were monitored at 24h, 48h, 72h and 96h after cisplatin administration using IVIS lumina bioimaging system.

2.17 Statistical analysis

Statistical analysis was performed using analysis of variation (ANOVA).

Where statistical significance was found, an unpaired Student's *t*-test was conducted between two groups. All analysis was performed by using

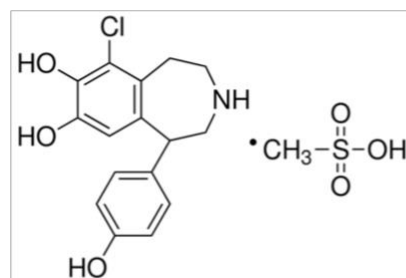
GraphPad Prism (GraphPad, San Diego, CA, USA). Significance was defined as $p < 0.05$.

Results

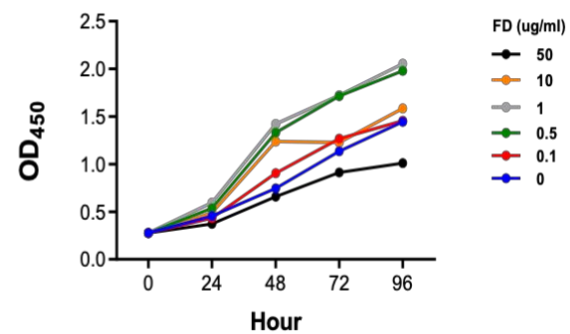
3.1 Effects of FD on MSC viability.

First, an optimal concentration of FD was determined, since ROS production can be increased due to autogenous enzymatic oxidation under higher concentration ($>10\mu\text{M}$) [49, 50]. When MSCs were treated with 0.1 to 1.0 $\mu\text{g/mL}$ of FD, the viability was increased. On the other hand, when FD was treated at a concentration of 50.0 $\mu\text{g/mL}$, it was judged that it was toxic because the survival rate decreased rather than control group (Figure 1b). In addition, to find the optimal concentration, I experimented for 24-72 h at more detailed concentrations of 1, 3 and 5 $\mu\text{g/mL}$. In the FD-treated group, cell viability increased at all concentrations as time increased. It showed similar results. Therefore, it was determined as the intermediate concentration of 3 $\mu\text{g /ml}$ (Figure 1c-e).

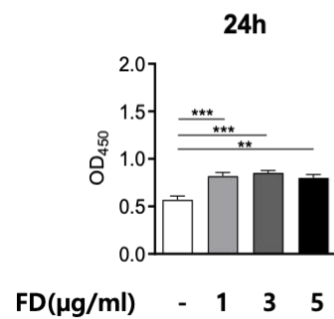
a



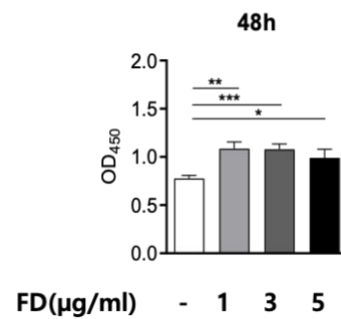
b



c



d



e

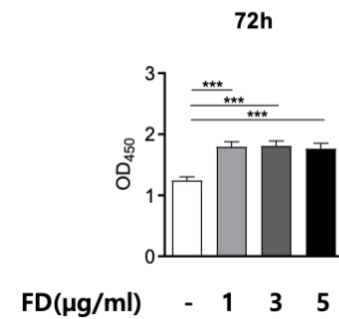


Figure 2. Chemical structure of FD and effects of FD on MSC viability. **a)** chemical structure of FD. **b)** hUC-MSCs were treated with various concentrations of FD for 0-96h. To determine the optimal concentration, we proceeded with a more detailed concentration for **c)** 24 h, **d)** 48 h, **e)** 72 h. All data are expressed as mean \pm standard deviation (SD) from three replications *: $p < 0.05$, **: $p < 0.01$ and ***: $p < 0.005$

3.2 Comparison of characteristics of mesenchymal stem cell.

Immunophenotypic characterization.

According to the International Society of Cellular Therapy (ISCT), in general, human MSCs show positive expression of more than 95 % of human markers CD73, CD90 and CD105, and CD11b, CD14, CD19, CD79a, CD34, Mesenchymal stem cells showing a negative expression of 2 % or less for CD45 and HLA-DR are defined as the minimum criterion requirement [4]. The surface markers of MSCs were identified by flow cytometry. Both MSCs and FD-primed MSCs showed positive expression patterns for CD73, CD90, and CD105, and negative expression patterns for CD34. Through this, it was confirmed that the immunophenotyping of hUC-MSCs did not change even after treatment with FD.

Differentiation potential

Stem cells can differentiate into more specialized cells [51, 52]. To examine the multilineage differentiation potentials of MSCs, *in vitro* differentiation of 7-9 passage MSCs and FD-primed MSCs into the osteogenic and chondrogenic lineages. After 14 days, we stained for analyzing the deposition of proteoglycan (Alcian blue), calcium (Alizarin Red) (Figure 2b). Compared to the MSCs, when FD-primed MSCs were differentiated into chondrocytes,

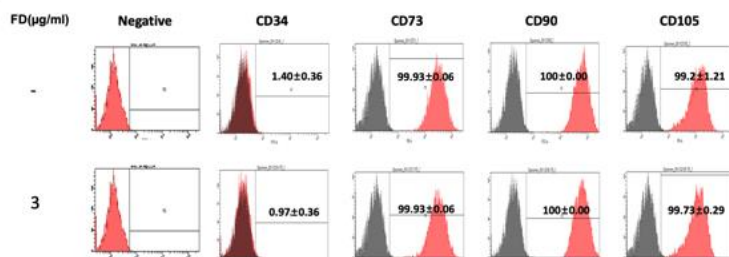
the deposition of proteoglycan, a glycosylated protein, was increased. As the proteoglycan increases, it becomes darker when stained with Alcian Blue. As a result of measuring absorbance at a wavelength of 620 nm, FD-primed MSCs were about 2.16 times higher than that MSCs group (Figure 2e). Compared to the MSCs, when FD-primed MSCs were differentiated into osteocytes, the calcium deposition was increased. Accordingly, the degree of dyeing with alizarin red became darker. As a result of measuring absorbance at a wavelength of 405 nm, the measured value was approximately 1.6 times higher than that of the MSCs group (Figure 2f). Through this, quantitatively confirmed results showed that FD-primed MSCs improved the ability to differentiate into chondrocytes and osteocytes.

CFU assay

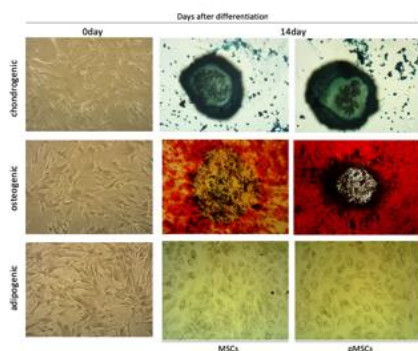
Hemopoietic contamination, the presence of macrophages, endothelial cells, and lymphocytes, which also adhere to plastic, is often present in the early BM monolayer[52]. However, only fibroblast-like spindle-shaped cells proliferate and form colonies termed colony-forming unit-fibroblasts (CFU-Fs), which are representative of the more highly proliferative cells in MSCs[53]. To evaluate the self-renewal ability of cells, a colony-forming unit assay (CFU assay) was performed (Figure 2d). FD-primed MSCs group showed a higher value by about 1.90 times than the MSCs group (Figure 2g).

Through this, it was confirmed that pretreatment with FD increased the self-renewal ability of hUC-MSC.

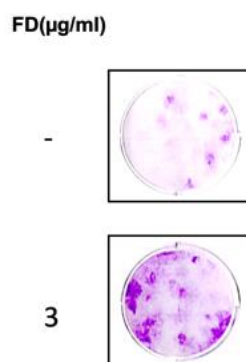
a



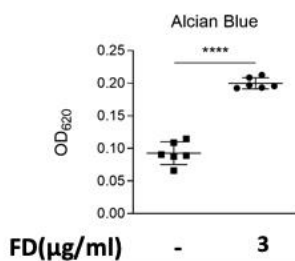
b



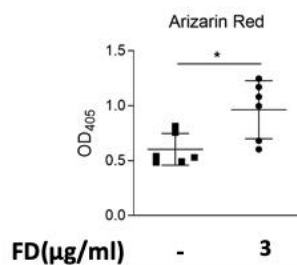
c



d



e



f

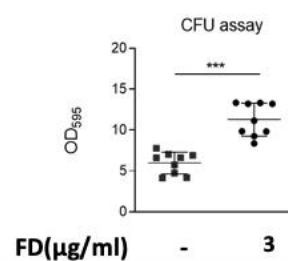


Figure 3. phenotype, multilineage differentiation and CFU-F colony formation of MSCs and FD-primed MSCs. a) Flow cytometric analysis of MSC and FD-primed MSCs. Panels were selected based on previous literature describing positive and negative markers for MSC. **b)** An optical micrograph after staining of cells that did not induce differentiation and induced differentiation. Magnification, unstained $\times 100$, stained $\times 40$. **c)** CFU-F assay in MSCs and pMSCs. The degree of differentiation into **d)** chondrocytes and **e)** osteocytes in Figure b was quantitatively shown. **f)** colony forming unit in Figure d was quantitatively measured. All data are expressed as mean \pm standard deviation (SD) from 3-6 replications *: $p < 0.05$, ***: $p < 0.005$, ****: $p < 0.0001$

3.3 FD-primed MSCs alleviated H₂O₂-induced apoptosis

Oxidative stress caused by hydrogen peroxide H₂O₂ leads to cell death and has been implicated in the pathogenesis. However, regulation of the NRF2/HO-1 pathway can reduce H₂O₂-induced oxidative damage in human melanocytes[54]. Therefore, to determine whether MSCs can also protect against H₂O₂ induced apoptosis through the NRF2/HO-1 pathway, and the experiment was conducted through CCK-8.

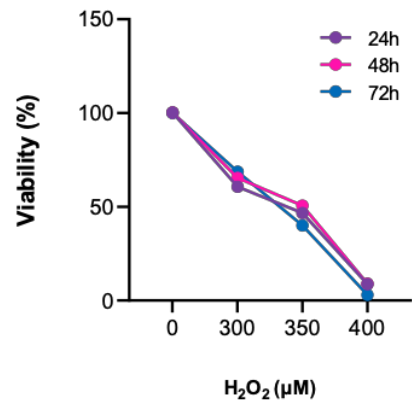
H₂O₂ has been reported to induce apoptosis of MSCs at various concentrations and time-points[55]. To find an appropriate concentration, H₂O₂ was treated for 24-72 hours by concentration (300-400 μ M) to evaluate the cell viability (Figure 3a). After inducing cell damage of hUC-MSC with 300 μ M of H₂O₂ and treating it with FD, the viability of cells was measured. The absorbance results showed that (-/+) group decrease in cell viability at 12h, 24 h, and 48 h. however, After 24 h, viability was recovered as much as (-/-) group by FD treatment (Figure 3b-d). Through this, it was confirmed that when 1.0 μ g/mL or 3.0 μ g/mL of FD was treated, damaged cells were recovered. (-/-) group was not treated with FD and H₂O₂, (-/+) group was treated with only H₂O₂, In the (+/1) and (+/3) groups, the concentration of FD 1 or 3 μ g/mL and hydrogen peroxide were administered simultaneously.

To confirm whether the FD pretreatment group reduced cell apoptosis, viability was observed by flow cytometry (Figure 3e). The (-/-)

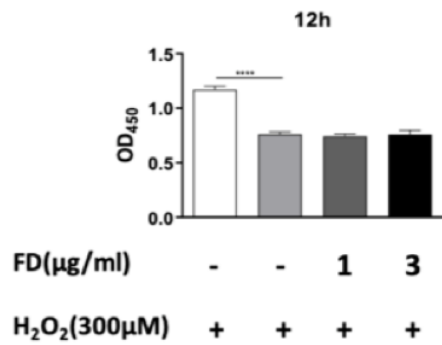
group showed a survival rate of about 80 %. In the (-/+), The proportion of early apoptotic cells (Annexin V+/PI-) was significantly increased following treatment with 300 μ M H₂O₂ for 6 h. However, we confirmed that the (+/+) group increased cell viability to a level similar to that of the (-/-) group (Figure 3f). Based on these results, it was concluded that FD pretreatment could also protect cells from ROS damage.

(-/-): no H₂O₂, no FD, (-/+): only H₂O₂, (3/+): after FD pre-conditioning at 3 μ g/mL for 72 h, H₂O₂ 500 μ M for 6 h.

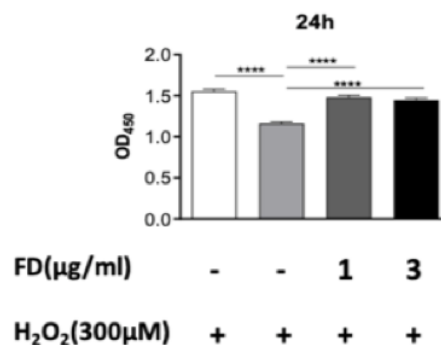
a



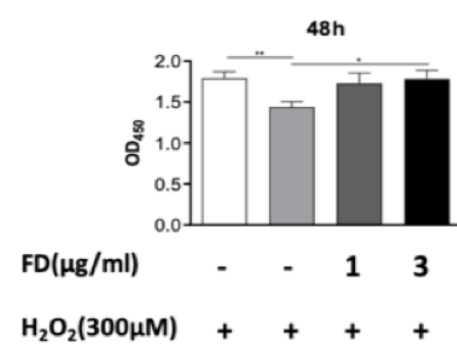
b



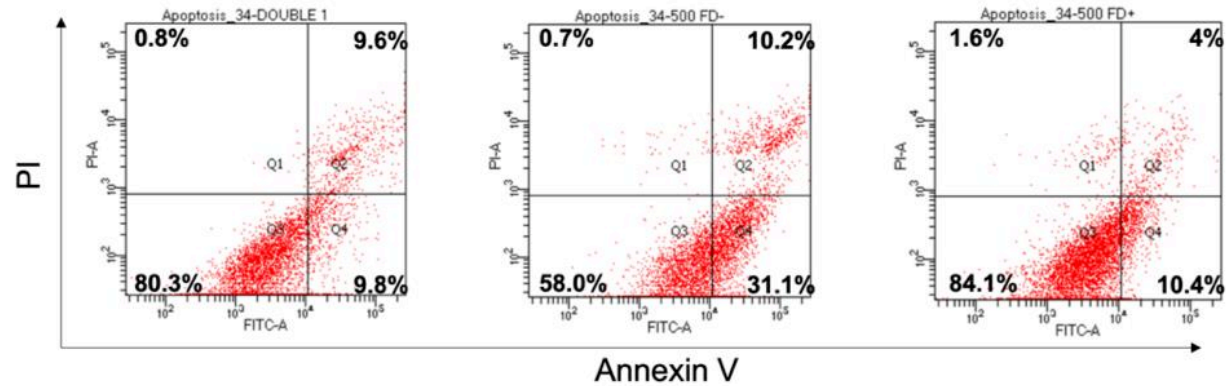
c



d

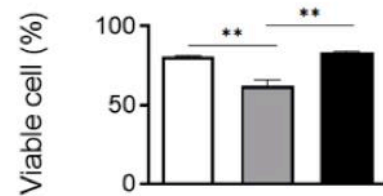


e



FD($\mu\text{g/ml}$)	-	-	3
H ₂ O ₂ (500 μM)	-	+	+

f



FD($\mu\text{g/ml}$)	-	-	3
H ₂ O ₂ (500 μM)	-	+	+

Figure 4. FD significantly reduced H₂O₂ induced apoptosis in hUC-MSCs. Effect of FD and H₂O₂ on cell viability detected by CCK-8. **a)** The viability of cells treated with 300-400 μ M H₂O₂. **b)** hUC-MSCs were treated simultaneously with 1 or 3 μ g/mL FD and H₂O₂ 300 μ M for **b)** 12 h **c)** 24 h **d)** 48 h. Effect of FD and H₂O₂ on cell viability detected by flow cytometry **e)** Cells were primed w/wo 3 μ g/mL FD for 72 h prior to exposure to H₂O₂. The stage of cell death was assessed by Annexin V-FITC/PI staining kit. These plots can be divided in four regions corresponding to : 1) viable cells which are negative to both probes (PI/FITC -/-; Q3); 2) apoptotic cells which are PI-negative and Annexin positive (PI/FITC -/+; Q1); 3) late apoptotic cells which are PI and Annexin positive (PI/FITC +/+; Q2); 4) necrotic cells which are PI-positive and Annexin negative (PI/FITC +/-; Q4). **f)** flow cytometry analysis is shown quantitatively. All data are expressed as mean \pm standard deviation (SD) from 3 replications *: $p < 0.05$, **: $p < 0.01$, ****: $p < 0.0001$

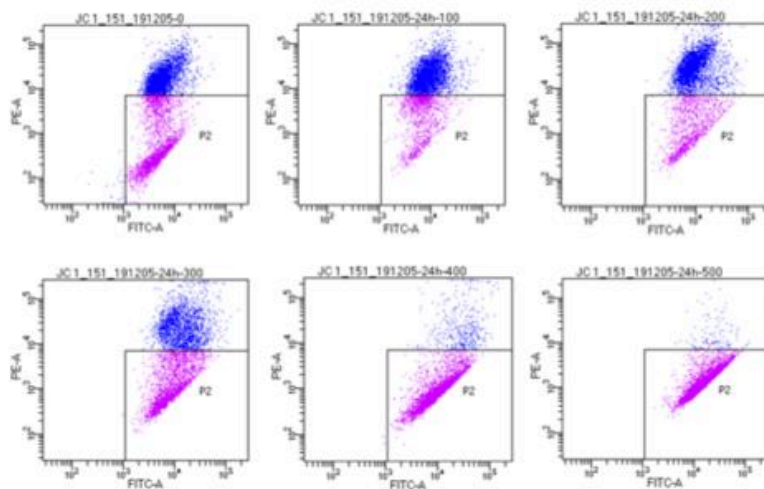
3.4 FD-primed MSCs maintain Ψ_m in ROS

The accumulation of ROS beyond the anti-oxidant function in the cell decreases the mitochondrial membrane potential (MMP), which is an indicator of the homeostasis of the electron transport chain, leading to a decrease in ATP production and apoptosis[56]. The maintenance of Ψ_m is related to scavenging efficiency of ROS [57]. Therefore, JC-1 dye was used to confirm whether FD-primed MSC could prevent the loss of Ψ_m . JC-1 dye penetrates the mitochondrial membrane well, which aggregates in the mitochondrial matrix and exhibits red fluorescence in normal cells. However, when the Ψ_m is reduced, JC-1 is converted to its monomer state, which exists green fluorescence in cytoplasm. After treatment with H₂O₂ at a concentration of 100-500 μ M for 24 h, it was confirmed that green fluorescence (Figure 4a) increased depending on the concentration. Based on these results, H₂O₂ at a concentration of 300 μ M was selected, which showed that the Ψ_m was a moderately reduced level. After appropriate treatment, the (-/-), (-/+) and (3/+) group were JC-1 stained (Figure 4b). in (-/-) grup, the red aggregate/green ratio decreased to about 2.26 according to the decrease in Ψ_m . On the other hand, the red agglutination/green ratio of the (3/+) group was about 2.9, showing an increase in mitochondrial membrane potential at a level similar to that of (-/-) group (about 2.84) (Figure 4c). Through this, it was confirmed that FD-primed MSCs were not affected by the oxidative

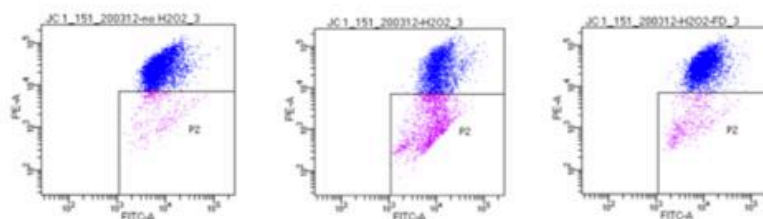
stress of H₂O₂ and the Ψ_m was not changed.

(-/-): no H₂O₂, no FD, (-/+): only H₂O₂, (3/+): after FD pre-conditioning at
3.0 μ g/mL for 72 h, H₂O₂ 300 μ M for 24 h

a



b



FD($\mu\text{g/ml}$)

-

-

3

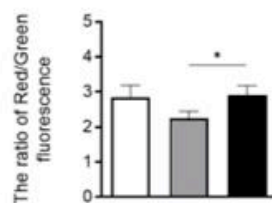
H₂O₂(300 μM)

-

+

+

c



FD($\mu\text{g/ml}$)

-

-

3

H₂O₂(300 μM)

-

+

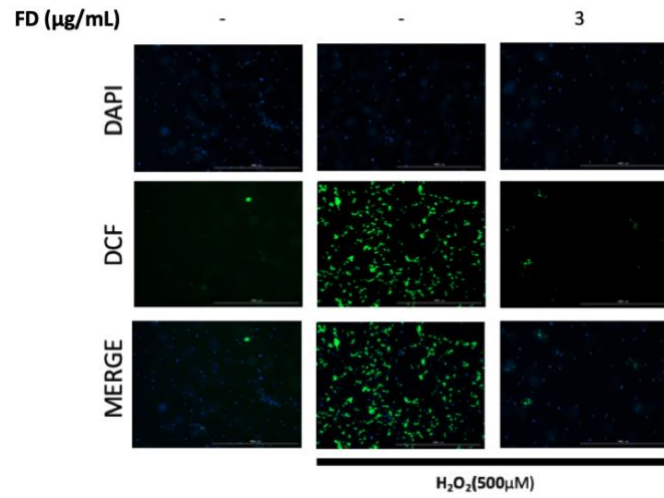
+

Figure 5. FD-primed MSCs maintain H₂O₂-mediated Ψ_m . **a)** Alteration in Ψ_m after H₂O₂ was treated at various concentrations. **b-c)** hUC-MSCs were pre-conditioned with 3 μ g/mL FD and then exposed to 300 μ M H₂O₂ for 24 h. The ratio of R/G fluorescence intensity was quantified. All data are expressed as mean \pm standard deviation (SD) from 3 replications *: $p < 0.05$

3.5 FD prevents intracellular ROS formation in MSCs

To examine the potential mechanisms underlying the protection of FD following H₂O₂ treatment, Dichlorofluorescein diacetate was used as a fluorescent probe to measure the change in the concentration of active oxygen in cells. DCF-DA, a non-fluorescent substance, enters the cell and is oxidized to DCF by ROS in the presence of peroxides related to hydrogen peroxide, resulting in green fluorescence. The result of A is a picture observed with a fluorescence microscope (Figure 5a), and the graph of (Figure 5b) is analyzed by FACS for quantification. It was confirmed that the DCF fluorescence intensity was increased by H₂O₂ treatment. However, the intensity was lowered in FD-primed MSC. Through quantitative analysis, it was found that the FD-primed MSCs group showed similar values to the normal group by scavenging intracellular ROS.

a



b

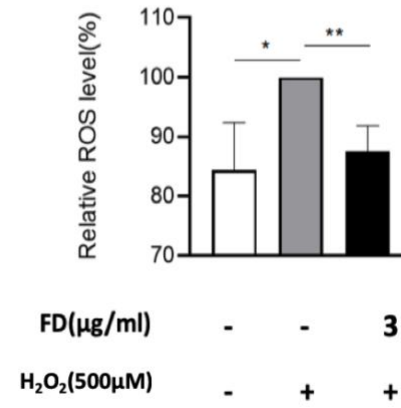
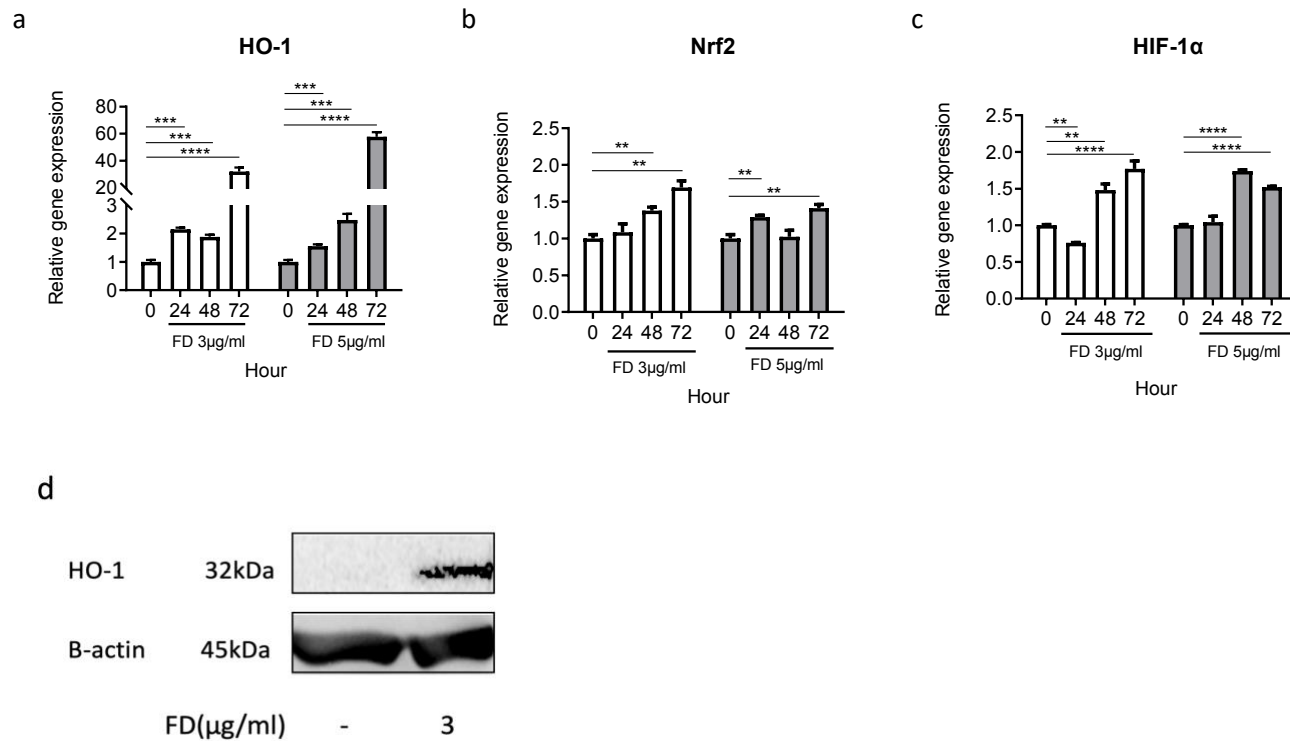


Figure 6. FD-primed MSCs scavenge intracellular ROS produced by H₂O₂ in MSCs. Cells were primed w/wo 3 μ g/mL FD for 72 h before exposure to H₂O₂. **a)** ROS production induced by H₂O₂ detected by H2DCFH-DA assay. The higher the ROS level, the lighter the fluorescence in the typical photos acquired by a fluorescence microscope. Magnification, $\times 40$. **b)** Quantitative analysis of DCF fluorescent intensity by flow cytometry. All data are expressed as mean \pm standard deviation (SD) from 3 replications *: $p < 0.05$, **: $p < 0.01$

3.6 FD-primed MSCs stimulate the expression of HIF-1 α , HO-1, NRF2

Activation of dopamine 1-like receptor is associated nitric oxide (NO) release[58]. NO stabilizes HIF-1 α protein. It also induces downstream genes of HIF-1 α under normoxia[59]. Enhanced HIF-1 α and HO-1 expression are two factors that participate in the renoprotective roles[60]. The anti-oxidant effects of D1-like receptors are eventually exerted by stimulating the anti-oxidant enzyme, heme oxygenase-1(HO-1), involves NRF2[61, 62]. To analyze the genes in which FD has an anti-oxidant effect on hUC-MSCs, gene candidates were identified through qRT-PCR. The anti-oxidant gene HO-1 was increased dose and time-dependently compared to the negative control group. The expression of HO-1 increased 31.96 and 57.81 times when 3 and 5 $\mu\text{g/ml}$ of FD was treated and cultured for 72 hours compared to the negative control (Figure 6a). Also, the expression of HO-1 protein is increased in FD-primed MSCs (Figure 6d).

In addition, the expression of NRF2, HIF-1 α was confirmed that the expression level of the group treated with FD increased to a certain level compared to the negative control group (Figure 6b-c). Through the measurement of the increased expression of HO-1, NRF2, and HIF-1 α , it was confirmed that the activity of the D1-like receptor stimulates anti-oxidant related gene.



e

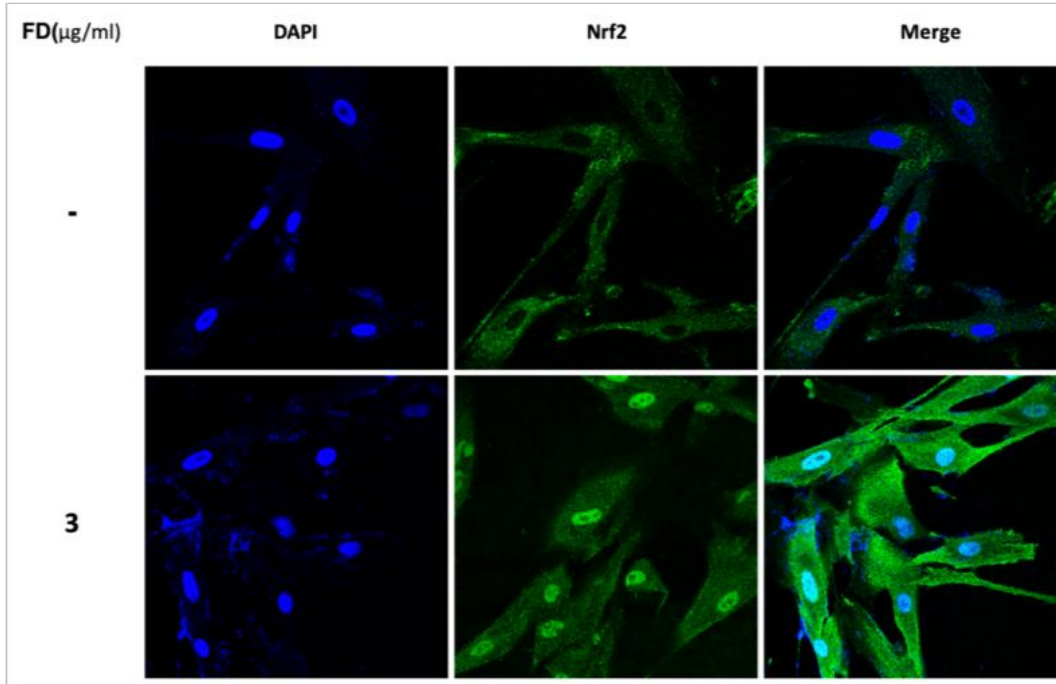


Figure 7. expression of hypoxia-inducible factor (HIF)-1 α , heme oxygenase (HO)-1, Nuclear factor erythroid-2-related factor 2 (NRF2). A-c) gene expression of HO-1, HIF-1 α , and NRF2. d) Immunoblot analysis of HO-1. β -ACTIN was used as loading control. e) The NRF2 stained positive cells were shown by immunofluorescence. All data are expressed as mean \pm standard deviation (SD) from 3 replications **: $p < 0.01$, *: $p < 0.005$, ****: $p < 0.0001$**

3.7 translocation of NRF2 into the nucleus by FD.

Nuclear factor erythroid 2-related factor 2 (NRF2) is the key transcription factor regulating anti-oxidant defense systems. Under normal conditions, Kelch-like ECH-associated protein 1 (Keap1) that represses NRF2 transcriptional activity[63]. During exposure to oxidative stress and Bardoxolone methyl (CDDO-me), the NRF2 is stabilization, following which NRF2 is translocated to the nucleus[64]. The accumulation of NRF2 in the nucleus induced expression of the downstream enzyme HO-1 that exert beneficial effects through the protection against oxidative stress, regulation of apoptosis, modulation of inflammation[65]. According to the results of markedly increased HO-1 gene expression and protein expression in Figure a, we confirmed through immunocytochemistry to observe whether the upstream protein, NRF2, translocation into the nucleus, a lot of accumulated in the nucleus when FD 24 h treatment was performed (Figure 6e).

Table 2. The antibody list used in this study

Target Protein	Primary antibody	Secondary antibody
HO-1	Heme Oxygenase 1 antibody (A-3): Santa Cruz (1:500)	Rabbit Anti-Mouse IgG H&L (HRP) (ab6728), abcam (1:10000)
β -Actin	Anti-beta Actin antibody (ab8227), abcam (1:2000)	Goat Anti-Rabbit IgG H&L (HRP) (ab721), abcam (1:10000)
BAX	BAX antibody (B-9): Santa Cruze (1:250-500)	Rabbit Anti-Mouse IgG H&L (HRP) (ab6728), abcam (1:10000)
β -Actin	Anti-beta Actin antibody (ab8227), abcam (1:2000)	Goat Anti-Rabbit IgG H&L (HRP) (ab721), abcam (1:10000)
p-CREB-1	p-CREB-1 (10E9), Santa cruz (1:500)	Rabbit Anti-Mouse IgG H&L (HRP) (ab6728), abcam (1:10000)
CREB-1	CREB-1 (D-12), Santa cruz (1:500)	Rabbit Anti-Mouse IgG H&L (HRP) (ab6728), abcam (1:10000)
β -Actin	Anti-beta Actin antibody (ab8227), abcam (1:2000)	Goat Anti-Rabbit IgG H&L (HRP) (ab721), abcam (1:10000)
p-ERK1/2	p-ERK 1/2 antibody (12D4): sc-81492, Santa cruz (1:1000)	Rabbit Anti-Mouse IgG H&L (HRP) (ab6728), abcam (1:10000)
ERK1/2	ERK 1/2 antibody (C-9): sc-514302, Santa cruz (1:1000)	Rabbit Anti-Mouse IgG H&L (HRP) (ab6728), abcam (1:10000)
β -Actin	Anti-beta Actin antibody (ab8227), abcam (1:2000)	Goat Anti-Rabbit IgG H&L (HRP) (ab721), abcam (1:1000)
p-AKT1/2/3	p-AKT1/2/3 antibody (B-5): sc-271966	Rabbit Anti-Mouse IgG H&L (HRP) (ab6728), abcam (1:10000)
β -Actin	Anti-beta Actin antibody (ab8227), abcam (1:2000)	Goat Anti-Rabbit IgG H&L (HRP) (ab721), abcam (1:1000)

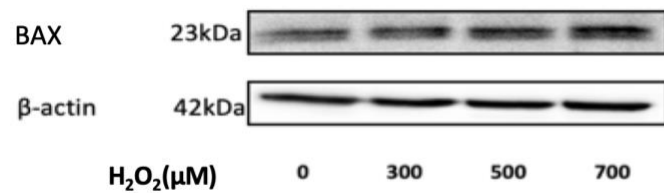
3.8 Identification of the signaling pathways

It is well known that the phosphorylation of CREB is quickly and temporarily increased by stimulation of the dopamine D1 receptor (D1DR) by dopamine[66]. The degree of phosphorylation of p-CREB-1 and CREB-1 over time of hUC-MSCs treated with FD (3.0 µg/mL) was measured by Western blot. hUC-MSCs treated with FD (3.0 µg/mL) showed the highest degree of phosphorylation of p-CREB-1 and CREB-1 after 0.5 hours. In addition, Western blot was performed to determine what the activity of the dopamine receptor is mediated through NRF2/HO-1 pathway. It was reported that DGMI (Diterpene ginkgolides meglumine injection) ameliorates I/R injury in rats by stimulating the PI3K/AKT-mediated NRF2 and CREB signaling pathway[67]. Another study reported that Eckol protect V79-4 cells against oxidative stress-induced cell death via activation of ERK and PI3K/AKT, which induce translocation NRF2[68]. Based on these literatures, Western blot was performed to determine what the activity of the dopamine receptor is mediated through NRF2/HO-1 pathway. The PI3K/AKT/CREB signaling pathway is to be an important regulator of neuron cell survival [69]. Referring to these results, Western blot was performed to confirm the phosphorylation of AKT and ERK. It was confirmed that both p-AKT/AKT and p-ERK/ERK significantly increased at 0.5 h (Figure 8a-b). Phosphorylation of CREB was also confirm (Figure 8c). Based on these

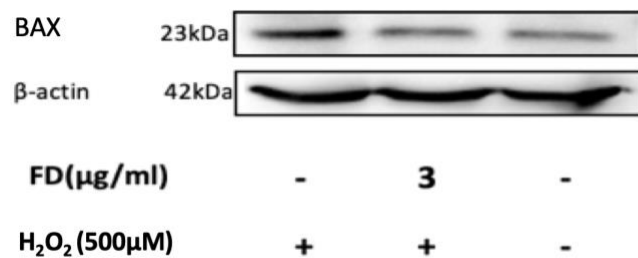
results, It implies that phosphorylation of AKT and ERK mediates the activation of NRF2 (Figure 6e) and CREB (Figure 8c) to reduced cell damage caused by ROS. H₂O₂ led to reduction of $\Delta\Psi_m$ and mitochondrial translocation of BAX and BAD[70]. BAX protein downregulated according to the expression of the Bcl-X_L protein by NRF-2[71]. I am confirmed that BAX expression was increased depending on the concentration of H₂O₂ (Figure 7a). However, BAX was downregulated by pretreatment with FD(Figure 7b-c).

In summary, our study showed that FD mitigated H₂O₂-induced damage on MSCs. Acting via the generation of cyclic AMP, upregulated ERK/CREB/BCL2 signaling. Another pathway activates PI3K/AKT, which promotes translocation of NRF2 into the nucleus, thereby increasing the expression of HO-1. Both pathways are involved in blocking the expression of BAX protein. It was confirmed that FD-primed MSCs prevented the reduction of MMP and eventually suppressed ROS and apoptosis (Figure 9).

a



b



c

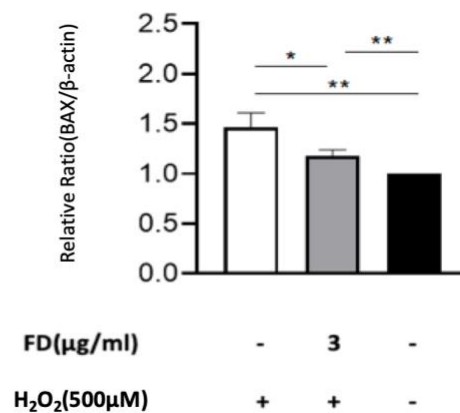


Figure 8. Effects of FD on H₂O₂-induced apoptosis related protein in mesenchymal stem cells. **a)** MSCs were treated with 300, 500, 700 μ M H₂O₂ for 6 h, and the expression levels of BAX (B-cell lymphoma 2 associated X protein) was detected by Western blot analysis. **b)** MSCs and FD-primed MSCs were treated with 500 μ M H₂O₂ for 6 h, and expression levels of BAX were detected by Western blotting. **c)** The relative expression of BAX against β -ACTIN (n=3). All data are expressed as mean \pm standard deviation (SD) from 3 replications *: $p < 0.05$, **: $p < 0.01$

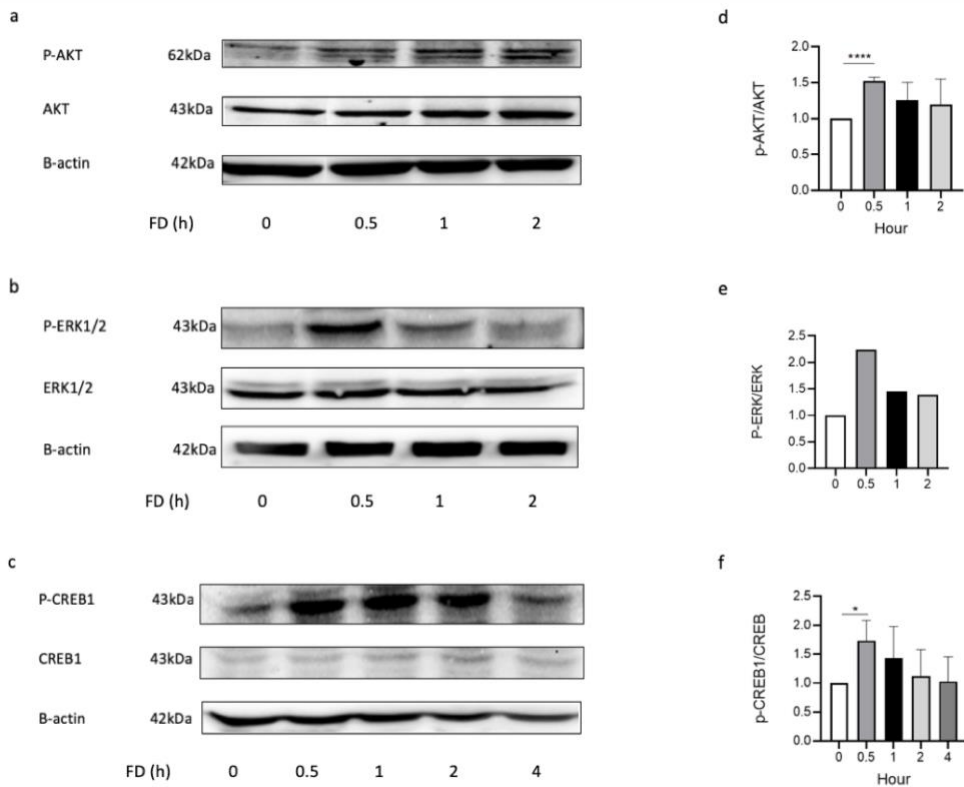


Figure 9. effects of FD on the phosphorylation of AKT, ERK, and CREB in MSCs. a) p-AKT/AKT (n=3). b) p-ERK/ERK(n=1). c) p-CREB/CREB (n=3). Cell lysates were prepared and analyzed by Western blot analysis to measure the relative amount of phosphorylated and total protein. **d-f)** The relative expression of BAX against β -ACTIN. All data are expressed as mean \pm standard deviation (SD) from 3 replications *: $p < 0.05$, ****: $p < 0.001$

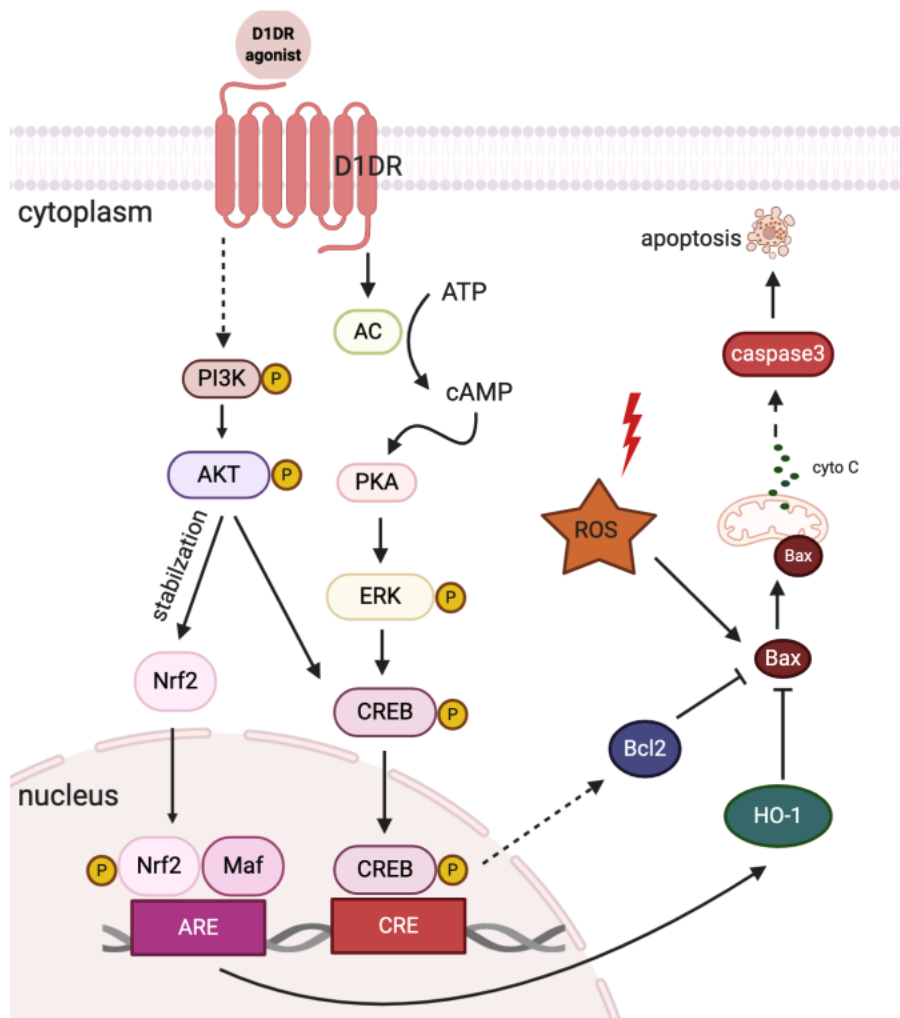
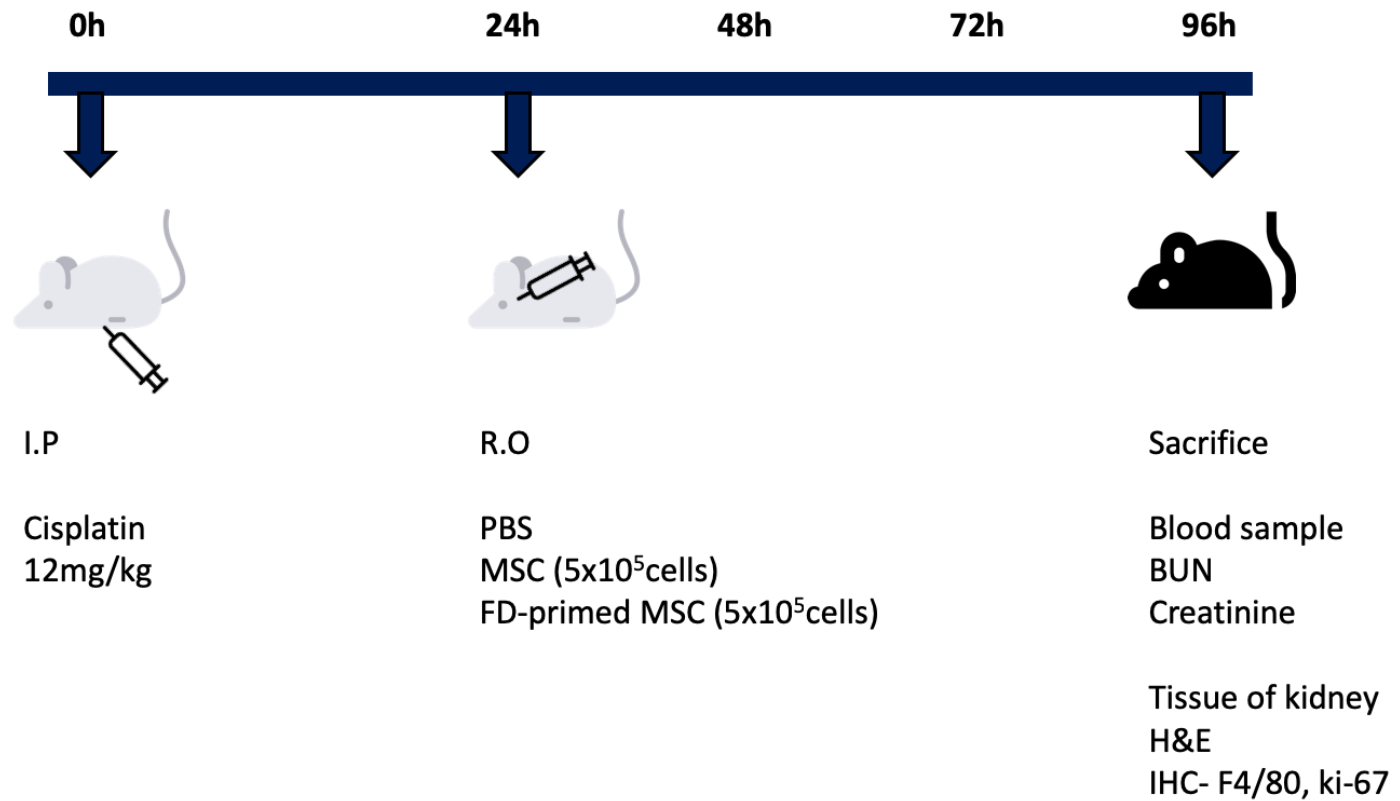


Figure 10. Schematic diagram describing the mechanism of FD in reducing ROS in MSCs.

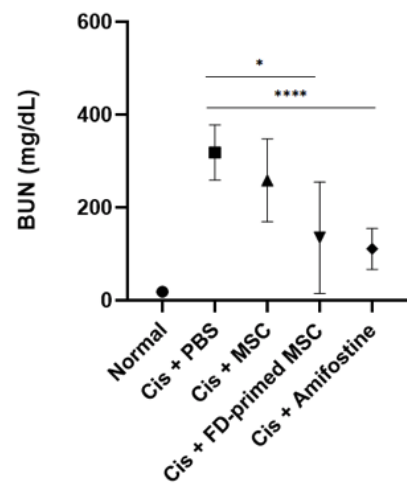
3. FD-primed MSCs alleviates cisplatin-induced AKI

The cisplatin rodent model was used to investigate the effect of FD-primed MSCs on acute kidney injury. The kidney morphology and histologic structures were significantly altered by cisplatin administration (Figure 11d-e). I discovered that the cortex of the injured kidney in FD-primed MSCs treated mice have a richer blood supply than that of the PBS-treated mice (Figure 11d). Cisplatin-treated animals showed an increased level of BUN and creatinine (Figure 10b-c), indicating that AKI had occurred. Notably, FD-MSCs-treated animals had an improved function in reducing AKI-induced renal dysfunction over those treated with MSCs (Figure 10b-c). Proliferation of interstitial fibroblasts is considered the feature of AKI[72]. I analyzed the expression of Ki-67 using IHC. The results demonstrated that proliferation of interstitial fibroblasts was increased in 4 days after cisplatin injection, and mice receiving FD-primed MSCs reduced the Ki-67⁺ cells (Figure 10f-g). I analyzed the effect of FD-primed MSCs in macrophages (F4/80⁺) to renal tissue at 4 days after cisplatin injection. Macrophage levels was significantly increased in mice treated PBS after cisplatin injection. Interestingly, mice receiving FD-primed MSCs treatment demonstrated limited infiltration macrophages (Figure 10i-j). Figure 10k shows fluorescent signal of MSCs and FD-primed MSCs after 24h-96h of cisplatin administration. No lethality was found up to 96h.

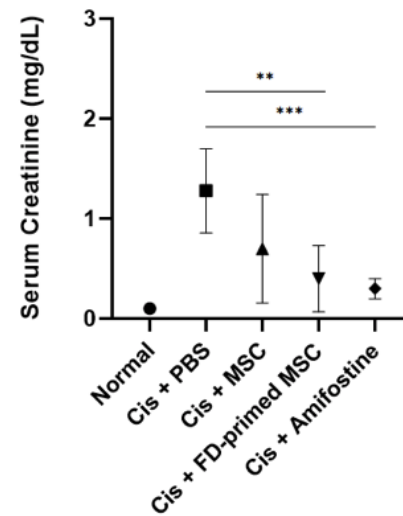
a



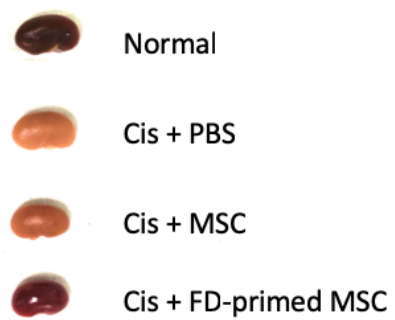
b



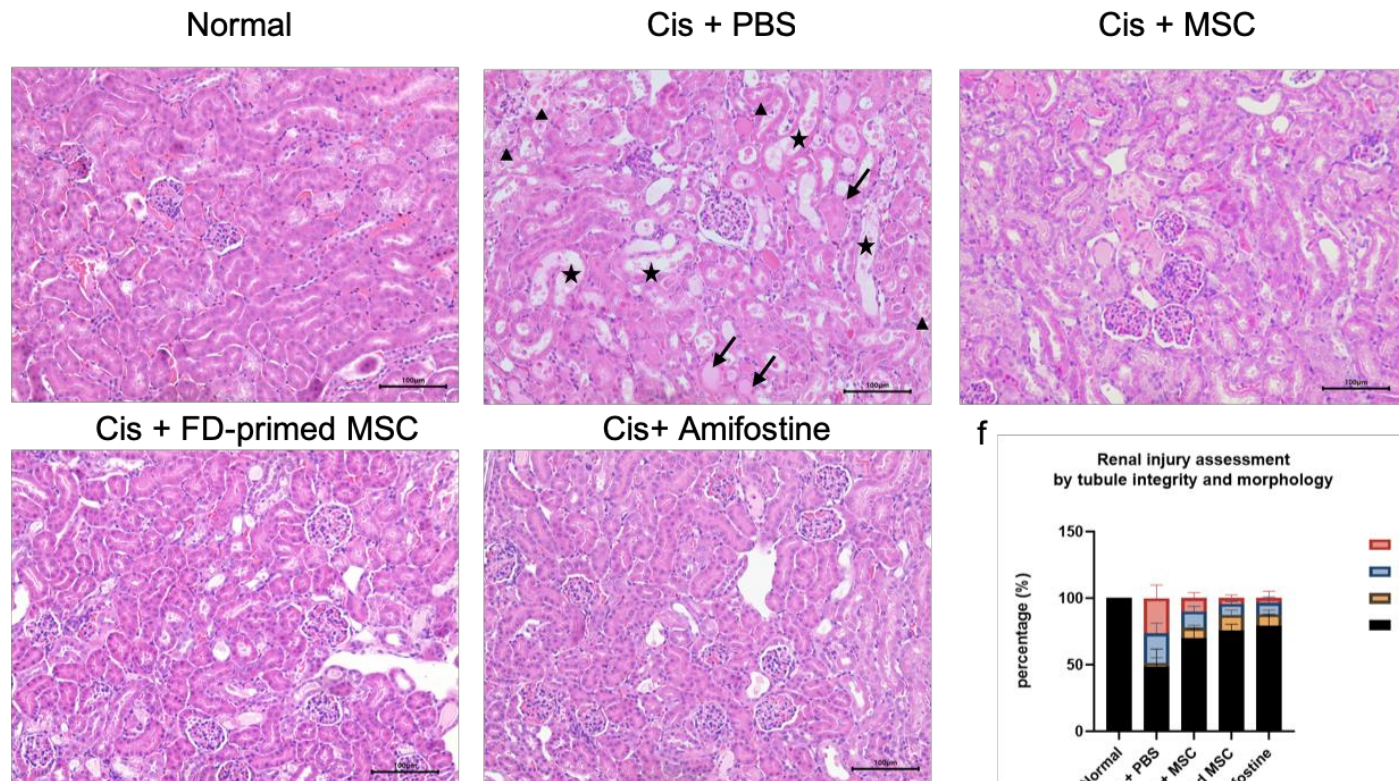
c



d

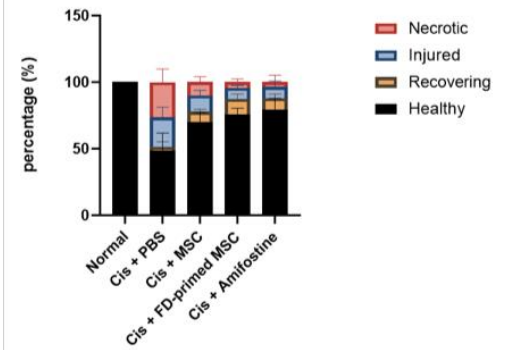


e

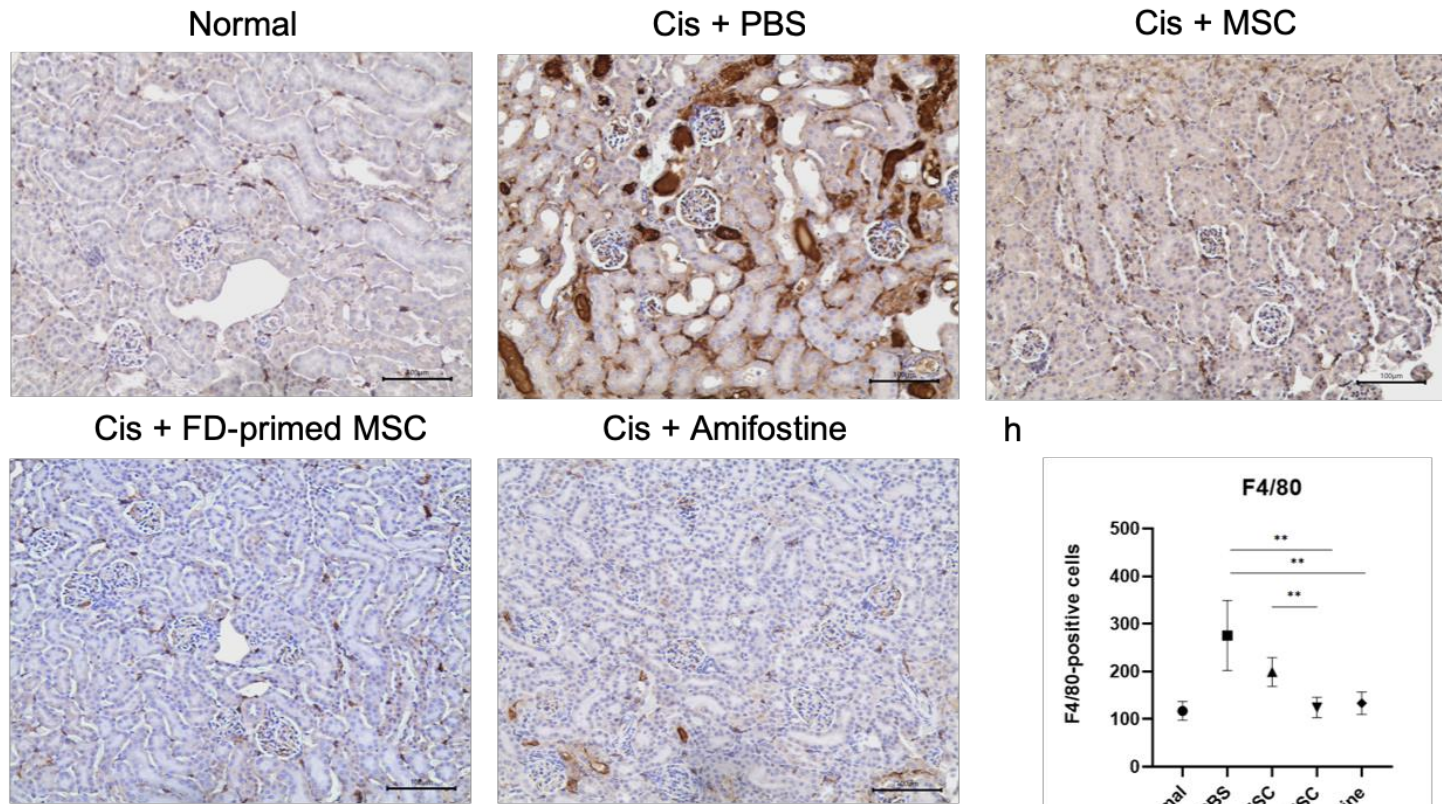


f

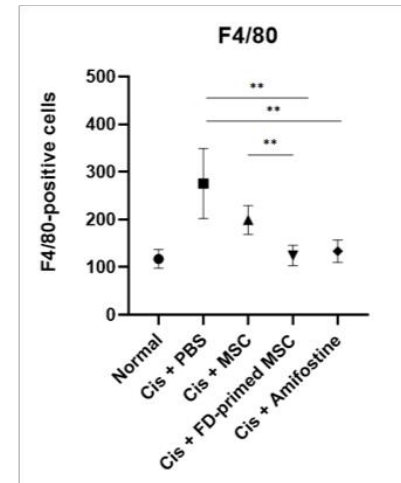
Renal injury assessment
by tubule integrity and morphology



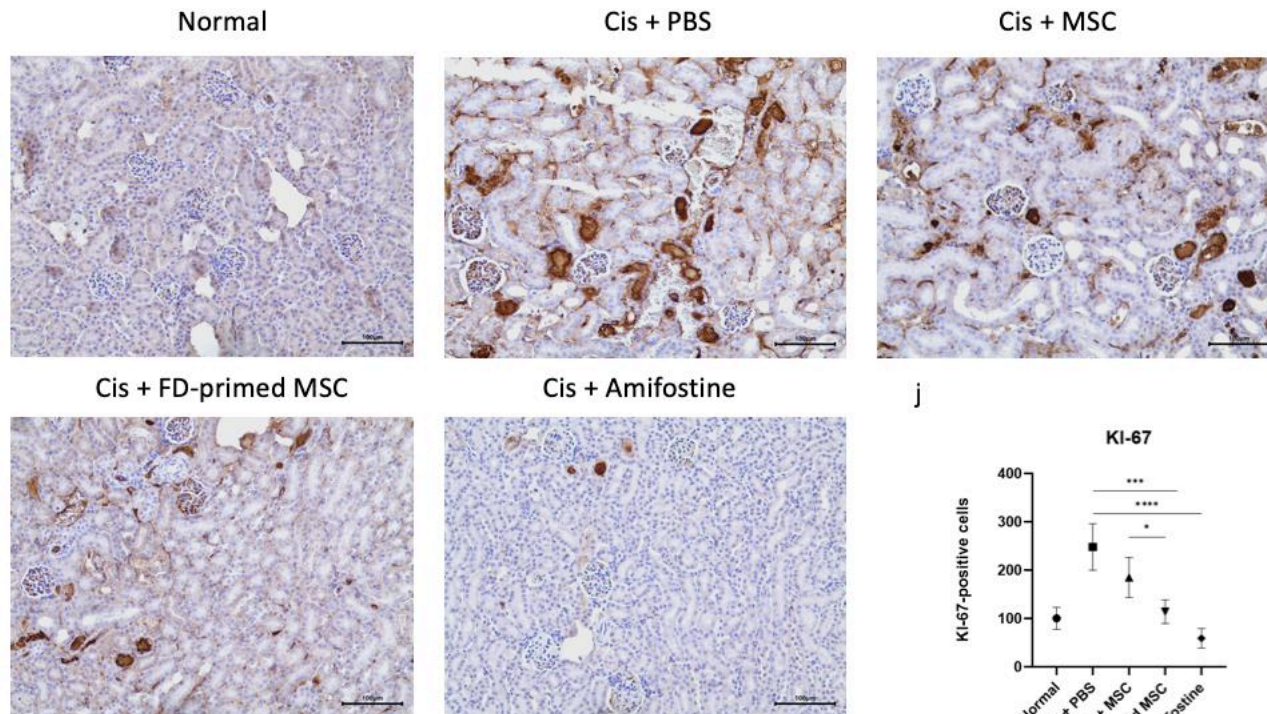
g



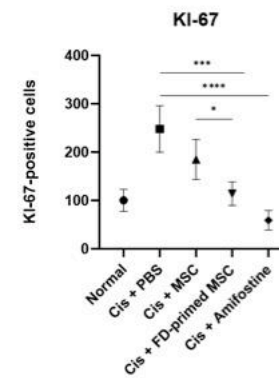
h



i



j



k

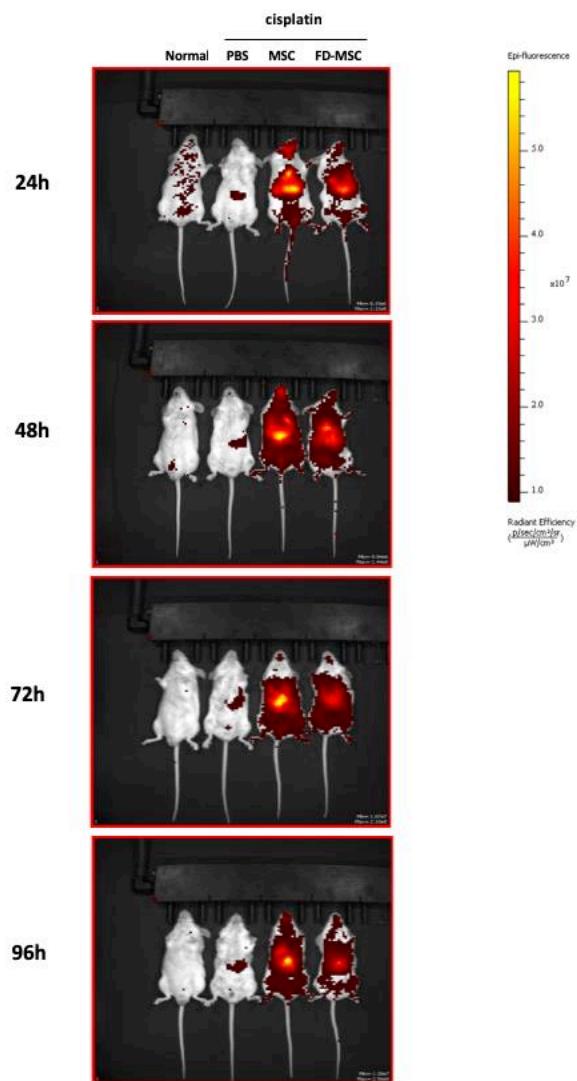


Figure 11. FD-primed MSCs improve renal recovery in an AKI. a)

Schematic representation of cisplatin-induced acute kidney injury and treatment with MSCs, FD-primed MSCs and amifostine. Renal function was evaluated by measuring **b)** serum creatinine and **c)** BUN (blood urea nitrogen). **d)** Representative macroscopic changes in kidney at 4 days after cisplatin injection. **e)** H&E staining. Arrowhead, asterisk and thin arrow indicate tubular epithelial recovering, injured and necrotic, respectively. **f)** Assessment of injury score in renal tubules. **g)** Immunohistochemical analysis of renal macrophages by staining with anti-F4/80 antibody. **h)** Immunohistochemical staining of proliferating tubular cells by staining with anti-Ki-67 antibody. Graph summarizing the F4/80 **i)** and Ki-67 **j)** positive cells. (original magnification x200, scale bar -100 μ m). **k)** In vivo hUC-MSCs bio-distribution. All data are expressed as mean \pm standard deviation (SD) from 5 replications *: $p < 0.05$, **: $p < 0.01$, ***: $p < 0.005$, ****: $p < 0.001$

4. Discussion

Acute kidney injury is characterized by a rapid reduction of renal function, mostly due to sudden blood hypoperfusion, toxic drugs, or microbiological infections[73]. If left untreated or etiologies are recurring, this condition can progress to chronic renal failure, which can lead to high morbidity.

Therefore, a therapeutic tool for resolving this disease is needed. Recent studies demonstrated that diuretics, dopamine, FD, EPO (Erythropoetin), and IGF-1 have produced promising results in preclinical studies, but evidence for use in humans is limited[28]. Due to its complex pathophysiology, one pharmacological agent often fails to improve outcomes. Thus, MSCs that can target various causes may become a promising measurement for AKI with such complex pathophysiology[74]. There have been many attempts to apply MSCs in AKI. For example, MSCs can stimulate renal recovery through engraftment and differentiation into renal cells[37]. Other study showed that kidney repair relied on the paracrine action of MSCs[75]. Despite its potential to rebuild renal function, poor cell survival *in vivo* limits its potential[76]. Accordingly, efforts to enhance the survival rate of MSCs are needed for successful cell therapy.

In mice lacking the dopamine D1 like receptor, hypertension appears, and it has been reported that the main cause for such phenotype is related to abrupt redox state in target cells[77]. A low concentration of dopamine D1 agonists has been demonstrated to have anti-oxidant effects in diverse cells[78-81]. Based on these results, we hypothesized that the anti-oxidant effect of MSCs could be increased by activating dopamine D1 like receptor by decreasing ROS.

Since previous studies showed that a high concentration of dopamine receptor agonist rather promotes the production of ROS[49, 50], I attempted to determine the optimal concentration of FD that can increase the overall performance of MSCs during *in vitro* culture. Thereafter, single protocols was established, e.g., treatment of 3 µg/mL of FD for 72 hours. This protocol led to an invariable expression profile of MSC markers. Moreover, differentiation study revealed that osteogenic and chondrogenic differentiation capacity was improved by FD. This results is in line with previous study that showed an increased osteogenic differentiation in MSCs[82].

To assess their physiological role *in vivo*, oxidative stress injury was given to MSC by H₂O₂. I found that treatment of simultaneous treatment of H₂O₂ and FD led to an enhanced recovery of apoptosis, compared with those are treated only with H₂O₂.

NRF2 is a transcription factor that promotes the expression of genes encoding anti-oxidant enzymes as well as cytoprotective effects[65]. HO-1 is one of the genes regulated by this gene[83]. This cytoprotective enzyme catalyzes the breakdown of heme, producing iron ion, CO and biliverdin. Biliverdin is then converted to bilirubin by the action of biliverdin reductase (BVR), which has anti-oxidant and anti-inflammatory effects[84]. In addition, Fe^{2+} and CO, the metabolites of heme by HO-1, also play an anti-apoptotic anti-inflammatory[65]. In our study, NRF2 protein was translocated to nucleus by FD. Also, the expression of HO-1, which is a well-known downstream gene of NRF2, was significantly upregulated. It was also confirmed that the well-known cytoprotective mechanism of NRF2/HO-1 is actually involved in the mitochondrial(intrinsic) pathway, which is consistent with the present study that confirmed a constant level of MMP(Ψ_m) by FD-priming. The maintenance of Ψ_m is related to scavenging efficiency of ROS [57]. FD-primed MSCs group showed similar values to the normal group by scavenging intracellular ROS.

Phosphorylation of CREB is known to stimulate the expression of the anti-apoptotic protein, BCL-2[85]. Conventionally, it is well known that the phosphorylation of CREB is quickly and temporarily increased by stimulation of the dopamine D1 receptor (D1DR) by dopamine[66]. Although the BCL-2 protein has not yet been identified, the reduction of the BAX

protein by FD was confirmed. These results suggest that BAX was reduced through the expression of BCL-2 by phosphorylated CREB. In addition, phosphorylation of AKT1/2/3 and ERK1/2 by FD was confirmed. Similarly, previous study showed that eckol protect V79-4 cells against oxidative stress-induced cell death via activation of ERK and PI3K/AKT, which induce translocation NRF2[68]. Another study showed that Kallikrein alleviates IRI through the ERK1/2-CREB-BCL2 pathway, while ERK1/2 inhibitor (U0126) inhibited this effect. Therefore, activation of ERK1/2 can ultimately activate CREB-BCL2 axis[85]. Based on these previous studies, it was possible to reduce the damage of cells through activation of CREB and NRF2 by phosphorylation of ERK1/2 or AKT1/2/3. In summary, Agonist of Dopamine D1 receptor, acting via the generation of cyclic AMP, upregulated ERK/CREB/BCL2 signaling. Another pathway activates PI3K/AKT, which promotes translocation of NRF2 into the nucleus, thereby increasing the expression of HO-1.

The present study demonstrated that stimulation of dopamine D1 receptor in MSCs reduced H₂O₂-induced cell damage by reducing intracellular ROS and maintaining of Ψ_m . This led to the downregulation of BAX protein involved in the intrinsic (mitochondria) pathway. As a result, apoptosis was significantly reduced in MSCs by activating NRF2 and CREB induced by PI3K/AKT and ERK. In addition, when FD-primed MSCs was

applied to cisplatin-induced AKI, it showed a better effect compared to the animals treated with non-primed MSCs.

Our results show that the expression of Ki-67 was increased by cisplatin, but significantly decreased by administration of FD-primed MSCs. Ki-67 is a nuclear antigen expressed during all phases except G0 in the cell cycle[86]. He et al. found that Ki-67 co-localization with Wnt4, whose function is known to be related to tubular repair[87]. Others found that kidney mononuclear phagocytes are implicated in pathogenesis and healing in mouse models of AKI[88]. Thus it can be assumed that the decreased expression of Ki-67 may represent a recovery phase in the mice model of cisplatin-induced AKI, albeit further study is needed to better confirm this finding.

Although the present study showed the feasibility of FD-primed MSCs in AKI, several issues should be addressed. Most of all, other biological mechanisms such as interaction with renal parenchymal tissue, the potential to differentiating into renal cells, should be clarified. Since MSCs produce diverse paracrine factors including extracellular vesicles and growth factors, analyzing change of their secretome is of importance to better understand the effect of dopamine D1 activation in MSCs.

References

1. Bianco, P., et al., *Bone marrow stromal stem cells: nature, biology, and potential applications*. Stem Cells, 2001. **19**(3): p. 180-92.
2. Zuk, P.A., et al., *Multilineage cells from human adipose tissue: implications for cell-based therapies*. Tissue Eng, 2001. **7**(2): p. 211-28.
3. Wexler, S.A., et al., *Adult bone marrow is a rich source of human mesenchymal 'stem' cells but umbilical cord and mobilized adult blood are not*. Br J Haematol, 2003. **121**(2): p. 368-74.
4. De Schauwer, C., et al., *Markers of stemness in equine mesenchymal stem cells: a plea for uniformity*. Theriogenology, 2011. **75**(8): p. 1431-43.
5. Dominici, M., et al., *Minimal criteria for defining multipotent mesenchymal stromal cells. The International Society for Cellular Therapy position statement*. Cytotherapy, 2006. **8**(4): p. 315-7.
6. Friedenstein, A.J., et al., *Stromal cells responsible for transferring the microenvironment of the hemopoietic tissues. Cloning in vitro and retransplantation in vivo*. Transplantation, 1974. **17**(4): p. 331-40.
7. Chamberlain, G., et al., *Concise review: mesenchymal stem cells: their phenotype, differentiation capacity, immunological features, and potential for homing*. Stem Cells, 2007. **25**(11): p. 2739-49.
8. Ghannam, S., et al., *Immunosuppression by mesenchymal stem cells: mechanisms and clinical applications*. Stem Cell Res Ther, 2010. **1**(1): p. 2.
9. Baltzer, A.W., et al., *Autologous conditioned serum (Orthokine) is an effective treatment for knee osteoarthritis*. Osteoarthritis Cartilage, 2009. **17**(2): p. 152-60.
10. Webster, R.A., et al., *The role of mesenchymal stem cells in veterinary therapeutics - a review*. N Z Vet J, 2012. **60**(5): p. 265-72.
11. Pachon-Pena, G., et al., *Obesity Determines the Immunophenotypic Profile and Functional Characteristics of Human Mesenchymal Stem Cells From Adipose Tissue*. Stem Cells Transl Med, 2016. **5**(4): p. 464-75.

12. Siegel, G., et al., *Phenotype, donor age and gender affect function of human bone marrow-derived mesenchymal stromal cells*. BMC Med, 2013. **11**: p. 146.
13. Amiri, F., A. Jahanian-Najafabadi, and M.H. Roudkenar, *In vitro augmentation of mesenchymal stem cells viability in stressful microenvironments : In vitro augmentation of mesenchymal stem cells viability*. Cell Stress Chaperones, 2015. **20**(2): p. 237-51.
14. Li, Q., Y. Wang, and Z. Deng, *Pre-conditioned mesenchymal stem cells: a better way for cell-based therapy*. Stem Cell Res Ther, 2013. **4**(3): p. 63.
15. Wei, H., et al., *Apoptosis of mesenchymal stem cells induced by hydrogen peroxide concerns both endoplasmic reticulum stress and mitochondrial death pathway through regulation of caspases, p38 and JNK*. J Cell Biochem, 2010. **111**(4): p. 967-78.
16. Lee, K.A., et al., *Analysis of changes in the viability and gene expression profiles of human mesenchymal stromal cells over time*. Cytotherapy, 2009. **11**(6): p. 688-97.
17. Xu, J., et al., *High density lipoprotein protects mesenchymal stem cells from oxidative stress-induced apoptosis via activation of the PI3K/Akt pathway and suppression of reactive oxygen species*. Int J Mol Sci, 2012. **13**(12): p. 17104-20.
18. Cruz, F.F. and P.R. Rocco, *Hypoxic preconditioning enhances mesenchymal stromal cell lung repair capacity*. Stem Cell Res Ther, 2015. **6**: p. 130.
19. Hu, C. and L. Li, *Preconditioning influences mesenchymal stem cell properties in vitro and in vivo*. J Cell Mol Med, 2018. **22**(3): p. 1428-1442.
20. Costantini, D., *Understanding diversity in oxidative status and oxidative stress: the opportunities and challenges ahead*. J Exp Biol, 2019. **222**(Pt 13).
21. Atashi, F., A. Modarressi, and M.S. Pepper, *The role of reactive oxygen species in mesenchymal stem cell adipogenic and osteogenic differentiation: a review*. Stem Cells Dev, 2015. **24**(10): p. 1150-63.
22. Cuevas, S., et al., *Renal dopamine receptors, oxidative stress, and hypertension*. Int J Mol Sci, 2013. **14**(9): p. 17553-72.
23. Murphy, M.B., C. Murray, and G.D. Shorten, *Fenoldopam: a selective peripheral dopamine-receptor agonist for the treatment of severe*

- hypertension*. N Engl J Med, 2001. **345**(21): p. 1548-57.
24. Yang, J., et al., *Renal Dopamine Receptors and Oxidative Stress: Role in Hypertension*. Antioxid Redox Signal, 2020.
 25. Abdelaziz, T.S., et al., *Preventing acute kidney injury and improving outcome in critically ill patients utilizing risk prediction score (PRAIOC-RISKS) study: A prospective controlled trial of AKI prevention*. J Nephrol, 2020. **33**(2): p. 325-334.
 26. Susantitaphong, P., et al., *World incidence of AKI: a meta-analysis*. Clin J Am Soc Nephrol, 2013. **8**(9): p. 1482-93.
 27. Singbartl, K. and M. Joannidis, *Short-term Effects of Acute Kidney Injury*. Crit Care Clin, 2015. **31**(4): p. 751-62.
 28. Khwaja, A., *KDIGO clinical practice guidelines for acute kidney injury*. Nephron Clin Pract, 2012. **120**(4): p. c179-84.
 29. Li, J.S. and B. Li, *Renal Injury Repair: How About the Role of Stem Cells*. Adv Exp Med Biol, 2019. **1165**: p. 661-670.
 30. Waikar, S.S., K.D. Liu, and G.M. Chertow, *Diagnosis, epidemiology and outcomes of acute kidney injury*. Clin J Am Soc Nephrol, 2008. **3**(3): p. 844-61.
 31. Landoni, G., et al., *Reducing mortality in acute kidney injury patients: systematic review and international web-based survey*. J Cardiothorac Vasc Anesth, 2013. **27**(6): p. 1384-98.
 32. *Notice*. Kidney International Supplements, 2012. **2**(1): p. 1.
 33. Qiu, Z., D. Zhou, and D. Sun, *Effects of human umbilical cord mesenchymal stem cells on renal ischaemia-reperfusion injury in rats*. Int Braz J Urol, 2014. **40**(4): p. 553-61.
 34. Rodrigues, C.E., et al., *Human umbilical cord-derived mesenchymal stromal cells protect against premature renal senescence resulting from oxidative stress in rats with acute kidney injury*. Stem Cell Res Ther, 2017. **8**(1): p. 19.
 35. Zhang, R., et al., *Resveratrol improves human umbilical cord-derived mesenchymal stem cells repair for cisplatin-induced acute kidney injury*. Cell Death Dis, 2018. **9**(10): p. 965.
 36. Al-Husseiny, F., et al., *Amniotic Fluid-Derived Mesenchymal Stem Cells Cut Short the Acuteness of Cisplatin-Induced Nephrotoxicity in Sprague-*

- Dawley Rats*. Int J Stem Cells, 2016. **9**(1): p. 70-8.
37. Herrera, M.B., et al., *Mesenchymal stem cells contribute to the renal repair of acute tubular epithelial injury*. Int J Mol Med, 2004. **14**(6): p. 1035-41.
 38. Qian, H., et al., *Bone marrow mesenchymal stem cells ameliorate rat acute renal failure by differentiation into renal tubular epithelial-like cells*. Int J Mol Med, 2008. **22**(3): p. 325-32.
 39. Liu, P., et al., *Enhanced renoprotective effect of IGF-1 modified human umbilical cord-derived mesenchymal stem cells on gentamicin-induced acute kidney injury*. Sci Rep, 2016. **6**: p. 20287.
 40. Zhang, R., et al., *Resveratrol improves human umbilical cord-derived mesenchymal stem cells repair for cisplatin-induced acute kidney injury*. Cell Death & Disease, 2018. **9**(10): p. 965.
 41. Liu, P., et al., *Enhanced renoprotective effect of IGF-1 modified human umbilical cord-derived mesenchymal stem cells on gentamicin-induced acute kidney injury*. Scientific Reports, 2016. **6**(1): p. 20287.
 42. Hoch, A.I., et al., *Differentiation-dependent secretion of proangiogenic factors by mesenchymal stem cells*. PLoS One, 2012. **7**(4): p. e35579.
 43. Tsubokawa, T., et al., *Impact of anti-apoptotic and anti-oxidative effects of bone marrow mesenchymal stem cells with transient overexpression of heme oxygenase-1 on myocardial ischemia*. Am J Physiol Heart Circ Physiol, 2010. **298**(5): p. H1320-9.
 44. Figueroa, F.E., et al., *Mesenchymal stem cell treatment for autoimmune diseases: a critical review*. Biol Res, 2012. **45**(3): p. 269-77.
 45. Bhat, A., et al., *Differential growth factor adsorption to calvarial osteoblast-secreted extracellular matrices instructs osteoblastic behavior*. PLoS One, 2011. **6**(10): p. e25990.
 46. Livak, K.J. and T.D. Schmittgen, *Analysis of relative gene expression data using real-time quantitative PCR and the 2(-Delta Delta C(T)) Method*. Methods, 2001. **25**(4): p. 402-8.
 47. Liu, Y.H., K. Li, and H.Q. Tian, *Renoprotective Effects of a New Free Radical Scavenger, XH-003, against Cisplatin-Induced Nephrotoxicity*. Oxid Med Cell Longev, 2020. **2020**: p. 9820168.
 48. Hesketh, E.E., et al., *Renal ischaemia reperfusion injury: a mouse model of*

- injury and regeneration*. J Vis Exp, 2014(88).
49. Cosentino, M., et al., *Dopaminergic modulation of oxidative stress and apoptosis in human peripheral blood lymphocytes: evidence for a D1-like receptor-dependent protective effect*. Free Radic Biol Med, 2004. **36**(10): p. 1233-40.
 50. Eibl, J.K., Z. Abdallah, and G.M. Ross, *Zinc-metallothionein: a potential mediator of antioxidant defence mechanisms in response to dopamine-induced stress*. Can J Physiol Pharmacol, 2010. **88**(3): p. 305-12.
 51. Gepstein, L., *Derivation and potential applications of human embryonic stem cells*. Circ Res, 2002. **91**(10): p. 866-76.
 52. Pittenger, M.F., et al., *Multilineage potential of adult human mesenchymal stem cells*. Science, 1999. **284**(5411): p. 143-7.
 53. Friedenstein, A.J., R.K. Chailakhjan, and K.S. Lalykina, *The development of fibroblast colonies in monolayer cultures of guinea-pig bone marrow and spleen cells*. Cell Tissue Kinet, 1970. **3**(4): p. 393-403.
 54. Jian, Z., et al., *Heme oxygenase-1 protects human melanocytes from H₂O₂-induced oxidative stress via the Nrf2-ARE pathway*. J Invest Dermatol, 2011. **131**(7): p. 1420-7.
 55. Facchin, F., et al., *Comparison of Oxidative Stress Effects on Senescence Patterning of Human Adult and Perinatal Tissue-Derived Stem Cells in Short and Long-term Cultures*. Int J Med Sci, 2018. **15**(13): p. 1486-1501.
 56. Rigoulet, M., E.D. Yoboue, and A. Devin, *Mitochondrial ROS generation and its regulation: mechanisms involved in H₂O₂ signaling*. Antioxid Redox Signal, 2011. **14**(3): p. 459-68.
 57. Brand, M.D., et al., *Mitochondrial superoxide and aging: uncoupling-protein activity and superoxide production*. Biochem Soc Symp, 2004(71): p. 203-13.
 58. Venkatakrishnan, U., C. Chen, and M.F. Lokhandwala, *The role of intrarenal nitric oxide in the natriuretic response to dopamine-receptor activation*. Clin Exp Hypertens, 2000. **22**(3): p. 309-24.
 59. Brune, B. and J. Zhou, *The role of nitric oxide (NO) in stability regulation of hypoxia inducible factor-1alpha (HIF-1alpha)*. Curr Med Chem, 2003. **10**(10): p. 845-55.

60. Yi, X., G. Zhang, and J. Yuan, *Renoprotective role of fenoldopam pretreatment through hypoxia-inducible factor-1alpha and heme oxygenase-1 expressions in rat kidney transplantation*. Transplant Proc, 2013. **45**(2): p. 517-22.
61. Armando, I., V.A. Villar, and P.A. Jose, *Dopamine and renal function and blood pressure regulation*. Compr Physiol, 2011. **1**(3): p. 1075-117.
62. George, L.E., M.F. Lokhandwala, and M. Asghar, *Novel role of NF-kappaB-p65 in antioxidant homeostasis in human kidney-2 cells*. Am J Physiol Renal Physiol, 2012. **302**(11): p. F1440-6.
63. Itoh, K., et al., *Keap1 represses nuclear activation of antioxidant responsive elements by Nrf2 through binding to the amino-terminal Neh2 domain*. Genes Dev, 1999. **13**(1): p. 76-86.
64. Liby, K., et al., *The synthetic triterpenoids, CDDO and CDDO-imidazolidine, are potent inducers of heme oxygenase-1 and Nrf2/ARE signaling*. Cancer Res, 2005. **65**(11): p. 4789-98.
65. Loboda, A., et al., *Role of Nrf2/HO-1 system in development, oxidative stress response and diseases: an evolutionarily conserved mechanism*. Cell Mol Life Sci, 2016. **73**(17): p. 3221-47.
66. Liu, F.C. and A.M. Graybiel, *Spatiotemporal dynamics of CREB phosphorylation: transient versus sustained phosphorylation in the developing striatum*. Neuron, 1996. **17**(6): p. 1133-44.
67. Zhang, W., et al., *Diterpene ginkgolides protect against cerebral ischemia/reperfusion damage in rats by activating Nrf2 and CREB through PI3K/Akt signaling*. Acta Pharmacol Sin, 2018. **39**(8): p. 1259-1272.
68. Kim, K.C., et al., *Up-regulation of Nrf2-mediated heme oxygenase-1 expression by eckol, a phlorotannin compound, through activation of Erk and PI3K/Akt*. Int J Biochem Cell Biol, 2010. **42**(2): p. 297-305.
69. Wang, Y., et al., *SMND-309 promotes neuron survival through the activation of the PI3K/Akt/CREB-signalling pathway*. Pharm Biol, 2016. **54**(10): p. 1982-90.
70. Circu, M.L. and T.Y. Aw, *Reactive oxygen species, cellular redox systems, and apoptosis*. Free Radic Biol Med, 2010. **48**(6): p. 749-62.
71. Nitire, S.K. and A.K. Jaiswal, *Nrf2-induced antiapoptotic Bcl-xL protein*

- enhances cell survival and drug resistance*. Free Radic Biol Med, 2013. **57**: p. 119-31.
72. Zhou, D., et al., *Early activation of fibroblasts is required for kidney repair and regeneration after injury*. FASEB J, 2019. **33**(11): p. 12576-12587.
 73. Basile, D.P., M.D. Anderson, and T.A. Sutton, *Pathophysiology of acute kidney injury*. Compr Physiol, 2012. **2**(2): p. 1303-53.
 74. Togel, F., et al., *Autologous and allogeneic marrow stromal cells are safe and effective for the treatment of acute kidney injury*. Stem Cells Dev, 2009. **18**(3): p. 475-85.
 75. Togel, F., et al., *Administered mesenchymal stem cells protect against ischemic acute renal failure through differentiation-independent mechanisms*. Am J Physiol Renal Physiol, 2005. **289**(1): p. F31-42.
 76. Burst, V.R., et al., *Poor cell survival limits the beneficial impact of mesenchymal stem cell transplantation on acute kidney injury*. Nephron Exp Nephrol, 2010. **114**(3): p. e107-16.
 77. Lu, Q., et al., *D5 dopamine receptor decreases NADPH oxidase, reactive oxygen species and blood pressure via heme oxygenase-1*. Hypertens Res, 2013. **36**(8): p. 684-90.
 78. Li, H., et al., *D1-like receptors regulate NADPH oxidase activity and subunit expression in lipid raft microdomains of renal proximal tubule cells*. Hypertension, 2009. **53**(6): p. 1054-61.
 79. Yu, Y., et al., *Neuroprotective effects of atypical D1 receptor agonist SKF83959 are mediated via D1 receptor-dependent inhibition of glycogen synthase kinase-3 beta and a receptor-independent anti-oxidative action*. J Neurochem, 2008. **104**(4): p. 946-56.
 80. Li, G.Y., et al., *The D(1) dopamine receptor agonist, SKF83959, attenuates hydrogen peroxide-induced injury in RGC-5 cells involving the extracellular signal-regulated kinase/p38 pathways*. Mol Vis, 2012. **18**: p. 2882-95.
 81. Yasunari, K., et al., *Dopamine as a novel antioxidative agent for rat vascular smooth muscle cells through dopamine D(1)-like receptors*. Circulation, 2000. **101**(19): p. 2302-8.
 82. Corrigan, M.A., et al., *Ciliotherapy Treatments to Enhance Biochemically- and Biophysically-Induced Mesenchymal Stem Cell Osteogenesis: A*

- Comparison Study*. Cell Mol Bioeng, 2019. **12**(1): p. 53-67.
83. Alam, J., et al., *Nrf2, a Cap'n'Collar transcription factor, regulates induction of the heme oxygenase-1 gene*. J Biol Chem, 1999. **274**(37): p. 26071-8.
84. Balla, G., et al., *Ferritin: a cytoprotective antioxidant strategem of endothelium*. J Biol Chem, 1992. **267**(25): p. 18148-53.
85. Shi, R., et al., *Tissue Kallikrein Alleviates Cerebral Ischemia-Reperfusion Injury by Activating the B2R-ERK1/2-CREB-Bcl-2 Signaling Pathway in Diabetic Rats*. Oxid Med Cell Longev, 2016. **2016**: p. 1843201.
86. Cuylen, S., et al., *Ki-67 acts as a biological surfactant to disperse mitotic chromosomes*. Nature, 2016. **535**(7611): p. 308-12.
87. He, Y.X., et al., *Wnt4 is significantly upregulated during the early phases of cisplatin-induced acute kidney injury*. Sci Rep, 2018. **8**(1): p. 10555.
88. Lever, J.M., et al., *Resident macrophages reprogram toward a developmental state after acute kidney injury*. JCI Insight, 2019. **4**(2).

국문초록

급성 신장 손상 (AKI) 은 전 세계적으로 주요한 건강 문제로 남아 있습니다. 그 이유는 높은 사망률, 이환율 및 치료 부족 등으로 인한 문제입니다. 최근 수십 년 동안 보고된 연구에 의하면 중간엽 줄기세포 (MSC) 가 AKI의 대체 치료수단이 될 수 있는 가능성을 보였습니다. 그러나 손상된 부위의 과도한 산화 스트레스로 인해 생체 내에서 세포의 생존율이 낮기 때문에 임상 치료 잠재력이 제한됩니다. 따라서 hUC-MSC 이식의 성공적인 전략은 산화 스트레스 유발 세포 사멸을 예방하는 것입니다. 선택적 도파민 수용체 1 작용제인 FD (Fenoldopam)는 항산화 효소인 NADPH 산화 효소를 억제하여 항산화 효과를 발휘하고 항산화 효소인 헴 산화 효소(heme oxygenase)를 자극하는 것으로 보고되었습니다. 그러나 산화 손상을 줄이는 데 있어 UC-MSC에 대한 FD의 영향은 아직 밝혀지지 않았습니다.

이 연구는 FD 에 의한 도파민 D1 수용체의 활성화가 MSC 의 산화 손상을 줄일 수 있는지의 대한 여부를 결정하는 것을 목표로합니다. 또한, 시스플라틴 유도 AKI 모델에서 급성 신기능

장애에서 FD-전처리 된 MSC 의 치료 효과를 평가하였습니다. 그 결과 FD 로 자극 된 MSC 가 증식, 분화능 및 자기 재생 능력에서 더 나은 결과를 보여 주었다는 것을 발견했습니다. 또한 H₂O₂ 처리에 의해 세포 손상은 활성 산소 종의 생성과 세포사멸로 이어집니다. 하지만 FD 처리에 의해 정도가 감소되는 것을 확인할 수 있었습니다. 생화학 적 분석은 Bcl-2- 연관 X 단백질 (BAX) 의 발현이 감소하고, PI3K / AKT 및 ERK1 / 2 경로를 자극하여 NRF2 및 CREB 를 활성화하여 미토콘드리아 막 전위 (Ψ_m)가 유지되었음을 보여 주었습니다. 또한 시스플라틴을 투여 한 후 마우스에서, 혈액 요소 질소 (BUN) 및 크레아티닌 (Crea) 수치, 근위세뇨관의 세포 괴사, 신장조직에서 Ki-67 및 F4 / 80 양성 세포가 증가했습니다. 그러나 FD-전처리 된 MSC 로 치료된 시스플라틴-유도 AKI 마우스는 위의 모든 지수에서 상당한 감소를 보였습니다. 결론적으로, FD-primed MSC 는 AKI 를 줄이는 대안이 될 가능성이 있습니다.